

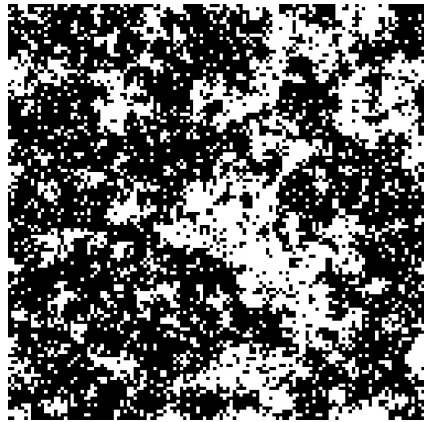
# PH40073: Mathematical Physics

## Part I: Phase Transitions

Lecturer: Habib Rostami

3 February 2025  
Semester 2: 2024/2025

<sup>1</sup>



## Literature

One motivation for supplying you with lecture notes for this course is the absence of a wholly ideal text book. However, it should be stressed that while these notes approach (in places) the detail of a book, the notes are not fully comprehensive and should be regarded as the ‘bare bones’ of the course, to be fleshed out via your own reading and supplementary note taking. To this end perhaps the most appropriate textbook is

- Lectures on Phase Transitions and the Renormalization Group, N. Goldenfeld (Addison Wesley)
- Renormalization Methods by W. D. McComb (Oxford University Press) 2007

You might also wish to dip into the introductory chapters of the following more advanced texts

- *Statistical Mechanics of Phase Transitions*, by J.M. Yeomans (Oxford).
- *The Critical Point* C. Domb, (Taylor and Francis).
- *The Theory of Critical Phenomena*, J.J. Binney, N.J. Dowrick, A.J. Fisher and M.E.J. Newman; (Oxford).

---

<sup>1</sup>Last update : March 3, 2025

# Contents

<b>1</b>	<b>Introduction</b>	<b>2</b>
<b>2</b>	<b>Background concepts</b>	<b>4</b>
2.1	Distinguishable vs indistinguishable particles . . . . .	6
<b>3</b>	<b>The Ising model: the prototype model for a phase transition</b>	<b>6</b>
3.1	The Ising model . . . . .	6
3.2	One-dimensional Ising chain . . . . .	8
3.2.1	Transfer matrix method . . . . .	9
<b>4</b>	<b>Mean Field Theory</b>	<b>10</b>
4.1	Mean field solution of the Ising model . . . . .	10
4.1.1	Order parameter scaling: zero H solution . . . . .	12
4.1.2	Magnetic susceptibility scaling: small H solution . . . . .	12
4.1.3	Magnetisation scaling with magnetic field . . . . .	13
4.1.4	Heat capacity scaling: zero H solution . . . . .	13
4.1.5	Correlation length scaling . . . . .	14
4.2	The Approach to Criticality . . . . .	14
4.3	Spontaneous symmetry breaking and phase transition . . . . .	15
4.3.1	Phase diagram: discontinuous (first-order) and continuous (second-order) transitions . . . . .	16
<b>5</b>	<b>Landau theory</b>	<b>17</b>
5.1	Landau theory for O(n) model . . . . .	20
5.2	Landau theory for nematic liquid crystals . . . . .	20
<b>6</b>	<b>Fluctuations and breakdown of mean-field theory</b>	<b>21</b>
6.1	Ginzburg criterion: when are fluctuations large? . . . . .	21
<b>7</b>	<b>The Static Scaling Hypothesis</b>	<b>22</b>
7.1	Experimental Verification of Scaling . . . . .	24
<b>8</b>	<b>The Renormalisation Group Theory of Critical Phenomena</b>	<b>25</b>
8.1	The critical point: A many length scale problem . . . . .	25
8.2	Methodology of the RG (conceptual viewpoint) . . . . .	26
8.2.1	Fluid-magnet universality . . . . .	28
8.2.2	Near critical scaling . . . . .	28
8.2.3	Universality classes . . . . .	28
8.3	Continuous scaling: $\beta$ -function . . . . .	29
<b>9</b>	<b>Methodology of the RG (effective coupling viewpoint)</b>	<b>31</b>
9.1	RG flows near a fixed point . . . . .	34
9.2	RG flow diagram: schematic discussion . . . . .	35

9.3	RG analysis of 1D Ising model . . . . .	37
9.4	RG analysis of 2D Ising model: High-T expansion approach . . . . .	39
9.5	RG analysis of percolation . . . . .	41
<b>10</b>	<b>Advanced topics (optional reading)</b>	<b>45</b>
10.1	Landau-Ginzburg theory . . . . .	45
10.2	Statistical field theory . . . . .	45
10.3	Goldstone's theorem . . . . .	46
10.4	Anderson-Higgs mechanism . . . . .	46

# 1 Introduction

A wide variety of physical systems undergo rearrangements of their internal constituents in response to the thermodynamic conditions to which they are subject. Two classic examples of systems displaying such phase transitions are the ferromagnet and fluid systems. As the temperature of a ferromagnet is increased, its magnetic moment is observed to decrease smoothly, until at a certain temperature known as the critical temperature, it vanishes altogether.

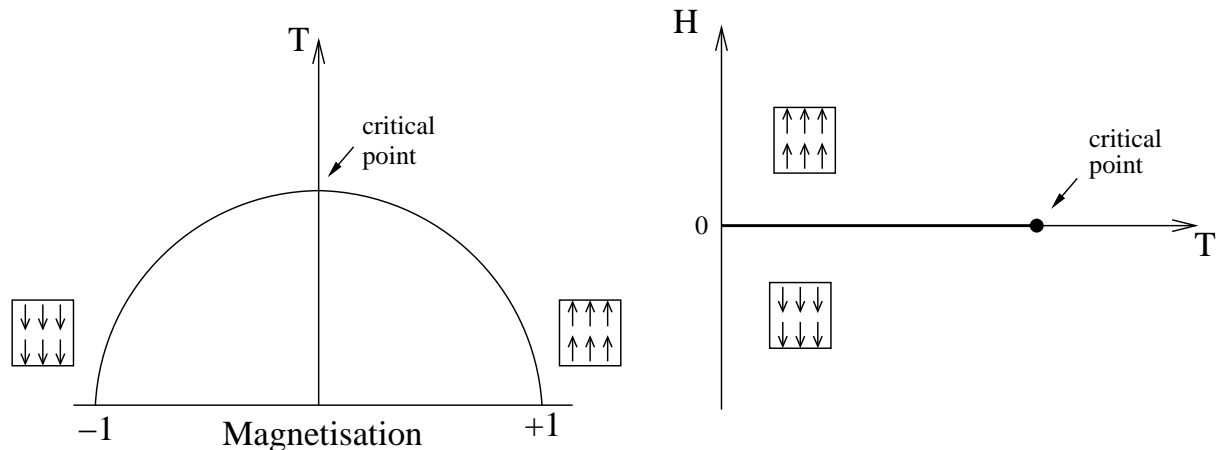


Figure 1: Phase diagram of a simple magnet (schematic)

Similarly, a change of state from liquid to gas can be induced in a fluid system (though not in an ideal gas) simply by raising the temperature. Typically the liquid-vapour transition is abrupt, reflecting the large density difference between the states either side of the transition. However the abruptness of this transition can be reduced by applying pressure. At one particular pressure and temperature the discontinuity in the density difference between the two states vanishes. These conditions of pressure and temperature serve to locate the critical point for the fluid.

**Example 1:** *Paramagnet-Ferromagnet transition.* A magnet can be seen as comprising magnetic dipoles (spins) on a crystal lattice capable of exchanging energy due to interaction with themselves and the background lattice. At high temperatures, the system is in the **paramagnetic phase**, where spins are randomly oriented, resulting in zero magnetisation. Below a critical temperature (Curie temperature),  $T_c$ , we have a **ferromagnetic phase** where spins tend to align along a specific direction, leading to a net magnetisation,  $M$ , even in the absence of an external field. This is a **continuous phase transition**, with magnetisation rising continuously from zero as the temperature decreases below  $T_c$ . Magnetisation serves as an **order parameter**, being zero in the disordered (paramagnetic) phase and non-zero in the ordered (ferromagnetic) phase. The onset of magnetisation in the three dimensional Ising ferromagnets

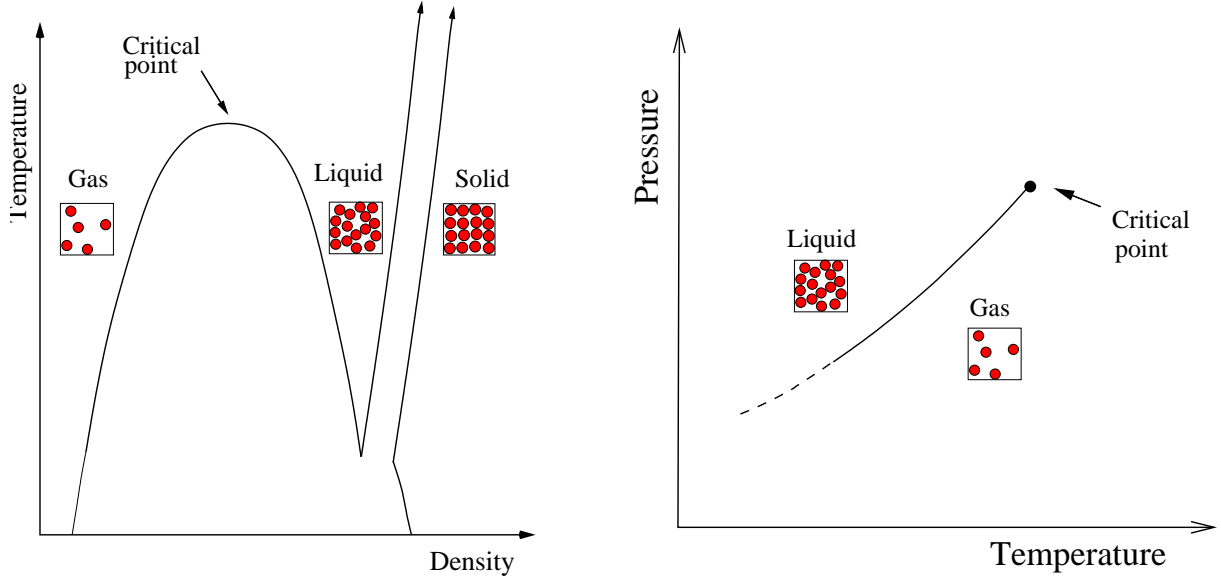


Figure 2: Phase diagram of a simple fluid (schematic)

(as well as antiferromagnet) in the limit of zero applied magnetic field, exhibits the following behaviour experimentally:

$$M \propto (T_c - T)^\beta, \quad \text{for } T < T_c \quad (1)$$

with  $\beta \sim 0.3$  in three dimensions. This result is valid in the limiting case as  $T \rightarrow T_c$ , from below as seen in Fig. 1.

**Example 2: Liquid-Gas transition.** In Fig. 2, a segment of a fluid's phase diagram is depicted, with axes representing temperature  $T$  and fluid density  $\rho$  in the fixed pressure  $P$  plane. Below the critical temperature  $T_c$ , the coexistence curve illustrates that increasing density at constant temperature necessitates passing through a two-phase region where both gas and liquid coexist. Above the critical point, a continuous transition from gas to liquid is possible with increasing density at constant temperature. In this scenario, there is no density where a mixture of liquid and gas coexists in the container. Even starting below the critical temperature  $T_c$ , it's always possible to transition directly from liquid to gas without encountering a two-phase region. This implies that distinguishing between a liquid and a gas is challenging. The coexistence curve near the critical point follow a power-law profile

$$|\rho_+(T) - \rho_-(T)| \propto (T_c - T)^{\beta'}, \quad \text{for } T < T_c \quad (2)$$

where  $\rho_{\pm}(T)$  are the density values at coexistence on the two branches of the curve below  $T_c$ , as illustrated in Fig. 2 (left panel). Surprisingly, the value of  $\beta'$  is remarkably close to the value of  $\beta$  associated with the magnetic critical point. This is not merely a coincidence; indeed, there is a profound **universal scaling** behaviour near the critical point that we will discuss in the course.

In the vicinity of a **critical point**, a system will exhibit a variety of remarkable effects known collectively as critical phenomena. Principal among these effects is the divergence of thermal response functions such as the specific heat and the fluid compressibility or magnetic susceptibility. It transpires that the origin of the singularities in these quantities can be traced to large-length-scale co-operative effects between the microscopic constituents of the system. The recalcitrant problem posed by the critical region is how best to incorporate such collective effects within the framework of a rigorous mathematical theory that affords both physical insight and quantitative explanation of the observed phenomena. This matter has been (and still is!) the subject of intense theoretical activity.

The importance of the critical point stems largely from the fact that many of the phenomena observed in its vicinity are believed to be common to a whole range of apparently quite disparate physical systems. Systems such as liquid mixtures, superconductors, liquid crystals, ferromagnets, antiferromagnets and molecular crystals may display *identical behaviour near criticality*. This observation implies a profound underlying similarity among physical systems at criticality, regardless of many aspects of their distinctive microscopic nature. These ideas have found formal expression in the so-called “**universality hypothesis**” which, since its inception some 35 years ago, has enjoyed considerable success.

In this course, principal aspects of the contemporary theoretical viewpoint of **phase transitions and critical phenomena** will be reviewed. **Mean field theories of phase transitions** will be discussed and their inadequacies in the critical region will be exposed. The phenomenology of the critical region will be described including power laws, critical exponents and their relationship to scaling phenomena. These will be set within the context of the powerful **Renormalisation Group** technique. The notion of universality as a phenomenological hypothesis will be introduced and its implications for real and model systems will be explored.

## 2 Background concepts

In seeking to describe near-critical phenomena, it is useful to have a quantitative measure of the difference between the phases coalescing at the critical point: this is the role of the **order parameter**. In the case of the fluid, the order parameter is taken as the difference between the densities of the liquid and vapour phases. In the ferromagnet it is taken as the magnetisation. As its name suggests, the order parameter serves as a measure of the kind of orderliness that sets in when the temperature is cooled below a critical temperature.

Our first task is to give some feeling for the principles which underlie the ordering process. For a system at constant total energy  $U$ , the thermodynamic variable of interest is the entropy  $S$ , which can be calculated using Boltzmann’s entropy formula,

$$S = k_B \ln W \tag{3}$$

where  $k_B$  is called Boltzmann’s constant and  $W$  is the number of different microstates (distinct configurations) at that energy. However, we are instead mostly interested in systems at constant temperature (see the Stat Mech reminder if these terms and their connections are unclear to you). The probability  $P_a$  that a physical system at temperature  $T$  will have a particular microscopic arrangement (configuration), labelled  $a$ , of energy  $E_a$  is

$$P_a = \frac{1}{Z} e^{-E_a/k_B T} = \frac{1}{Z} e^{-\beta E_a} \tag{4}$$

where  $\beta = 1/k_B T$ . The prefactor  $Z^{-1}$  is the *partition function*: since the system must always have *some* specific arrangement, the sum of the probabilities  $P_a$  must be unity, implying that

$$Z = \sum_a e^{-E_a/k_B T} \tag{5}$$

where the sum extends over all possible microscopic arrangements.

In utilizing these equations, it is generally correct to suppose that the physical system evolves rapidly (on the timescale of typical observations) amongst all its allowed arrangements, sampling them with the probabilities prescribed by Eq. (4); the expectation value of any physical observable  $O$  will thus be given by averaging  $O$  over all the arrangements  $a$ , weighting each contribution by the appropriate probability:

$$\langle O \rangle = \frac{1}{Z} \sum_a O_a e^{-E_a/k_B T} \tag{6}$$

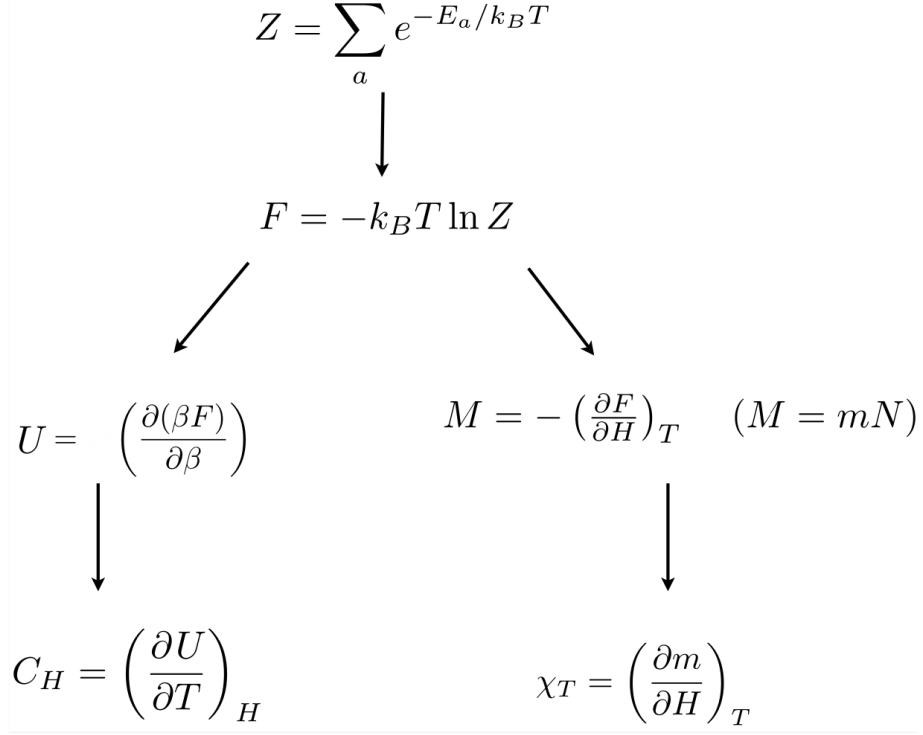


Figure 3: Relationships between the partition function and thermodynamic observables.

(Sometimes the notation  $\bar{O}$  is used to denote the exact same quantity as  $\langle O \rangle$ ). Sums like eq. 6 are not easily evaluated. Nevertheless, some important insights follow painlessly. Consider the case where the observable of interest is the order parameter, or more specifically the magnetisation of a ferromagnet.

$$m = \frac{1}{Z} \sum_a m_a e^{-E_a/k_B T} \quad (7)$$

From eq. 4, note that at very low temperature the system will be overwhelmingly likely to be found in its minimum energy arrangements (ground states). For the ferromagnet, these are the fully ordered spin arrangements having magnetisation +1, or -1.

Now consider the high temperature limit. The enhanced weight that the fully ordered arrangement carries in the sum of eq. 7 by virtue of its low energy, is now no longer sufficient to offset the fact that arrangements in which  $m_a$  has some intermediate value, though each carry a smaller weight, are vastly greater in number. A little thought shows that the arrangements which have essentially zero magnetisation (equal populations of up and down spins) are by far the most numerous. At high temperature, these disordered arrangements dominate the sum in eq. 7 and the order parameter is zero.

The competition between energy-of-arrangements weighting (or simply ‘energy’) and the ‘number of arrangements’ weighting (or ‘entropy’) is then the key principle at work here. The distinctive feature of a system with a critical point is that, in the course of this competition, the system is forced to choose amongst a number of macroscopically different sets of microscopic arrangements.

Finally in this section, we note that the probabilistic (statistical mechanics) approach to thermal systems outlined above is completely compatible with classical thermodynamics. Specifically, the bridge between the two disciplines is provided by the following equation

$$F = U - TS = -k_B T \ln Z \quad (8)$$

where  $F$  is called the Helmholtz free energy. All thermodynamic observables, for example the

magnetisation  $m$ , and response functions such as the specific heat or magnetic susceptibility are obtainable as appropriate derivatives of the free energy. For instance, utilizing eq. 5, one can readily verify (try it as an exercise!) that the average internal energy  $U$  is given by

$$U = -\frac{\partial \ln Z}{\partial \beta}, \quad (9)$$

where  $\beta = (k_B T)^{-1}$ . The relationship between other thermodynamic quantities and derivatives of the free energy are given in Fig. 3. Other variables we might consider are the entropy  $S$ , the pressure  $p$ , and the chemical potential  $\mu$ .

## 2.1 Distinguishable vs indistinguishable particles

For ideal gases, we can consider the particles to be indistinguishable (in the quantum mechanical sense). In a magnet, the spins are bound to a static atom in a crystal and therefore can be distinguished by their position. This difference leads to two different expressions for the partition function of a system composed of non-interacting particles (each particle described by partition function  $Z_1$ ), one for distinguishable particles and one for indistinguishable particles. For distinguishable particles, the  $N$ -particle partition function

$$Z_N = (Z_1)^N \quad (10)$$

because each particle contributes a factor of  $Z_1$ . For indistinguishable particles, this expression overcounts the number of configurations. Since for  $N$  particles, there are  $N!$  ways to order them, for a system of indistinguishable particles the partition function needs to be divided by  $N!$

$$Z_N = (Z_1)^N / N! \quad (11)$$

Note that these expressions are only valid when no interactions are included. With interactions, the total partition function cannot be written so simply in terms of single-particle partition functions.

## 3 The Ising model: the prototype model for a phase transition

In order to probe the properties of the critical region, it is common to appeal to simplified model systems whose behaviour parallels that of real materials. The sophistication of any particular model depends on the properties of the system it is supposed to represent. The simplest model to exhibit critical phenomena is the Ising model of a ferromagnet. Physical realisations of magnetic systems described by this model include layered ferromagnets such as  $K_2CoF_4$ , so the Ising model is of more than just technical relevance.

### 3.1 The Ising model

The Ising model envisages a regular arrangement of magnetic moments or ‘spins’ on, for example, an infinite plane. Each spin can take two values,  $s = +1$  (‘up’ spins) or  $s = -1$  (‘down’ spins) and is assumed to interact with its nearest neighbours according to the energy  $E_I$  (or Hamiltonian  $\mathcal{H}_I$ ) for a single configuration composed of many spins:

$$E_I = -J \sum_{\langle ij \rangle} s_i s_j - H \sum_i s_i \quad (12)$$

where  $J > 0$  measures the strength of the coupling between spins and the sum extends over nearest neighbour spins  $s_i$  and  $s_j$ .  $H$  is a magnetic field term which can be positive or negative (although for the time being we will set it equal to zero). The order parameter is simply the average magnetisation:

$$m = \frac{1}{N} \sum_i \langle s_i \rangle , \quad (13)$$

where  $\langle s_i \rangle = Z^{-1} \sum_{\{s\}} s_i e^{-\beta E\{s\}}$  means an average over configurations (statistical average).

The fact that the Ising model displays a phase transition was argued in sec. 2. Thus at low temperatures for which there is little thermal disorder, there is a preponderance of aligned spins and hence a net spontaneous magnetic moment (i.e. the system is ferromagnetic for  $J > 0$ ). As the temperature is raised, thermal disorder increases until at a certain temperature  $T_c$ , entropy drives the system through a continuous phase transition to a disordered spin arrangement with zero net magnetisation (ie. the system is paramagnetic). These trends are visible in configurational snapshots from computer simulations of the 2D Ising model (see Figure. 3.1). Although each spin interacts only with its nearest neighbours, the phase transition occurs due to cooperative effects among a large number of spins. In the neighbourhood of the transition temperature these cooperative effects engender fluctuations that can extend over all length-scales from the lattice spacing up to the correlation length.

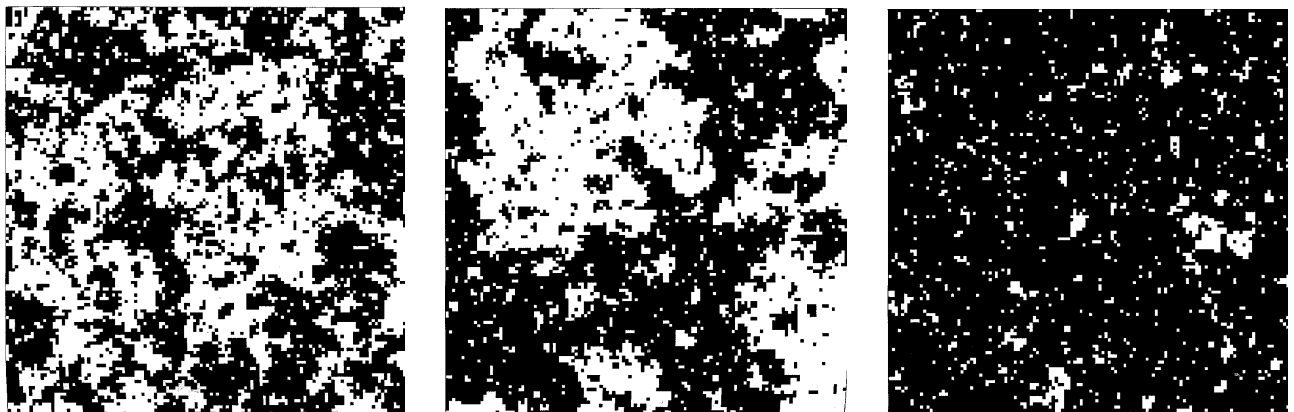


Figure 4: Configurations of the 2d Ising model. The patterns depict typical arrangements of the spins (white= $+1$ , black= $-1$ ) generated in a computer simulation of the Ising model on a square lattice of  $N = 512^2$  sites, at temperatures of (a)  $T = 1.2T_c$ , (b)  $T = T_c$  and (c)  $T = 0.95T_c$ . In each case only a portion of the system containing  $128^2$  sites in shown. The typical island size is a measure of the correlation length  $\xi$ : the excess of black over white (below  $T_c$ ) is a measure of the order parameter.

An interactive Java based Monte Carlo simulation of the Ising model can be found at <https://mattbierbaum.github.io/isng.js/> (also accessible via the Moodle page). By altering the temperature you will be able to observe for yourself how the spin arrangements change as one traverses the critical region. Pay particular attention to the configurations near the critical point. They have very interesting properties. We will return to them later!

Although the 2d Ising model may appear at first sight to be an excessively simplistic portrayal of a real magnetic system, critical point universality implies that many physical observables such as critical exponents are not materially influenced by the actual nature of the microscopic interactions. The Ising model therefore provides a simple, yet *quantitatively* accurate representation of the critical properties of a whole range of real magnetic (and indeed fluid) systems. This universal feature of the model is largely responsible for its ubiquity in the field of critical phenomena. We shall explore these ideas in more detail later in the course.

### 3.2 One-dimensional Ising chain

What about the one-dimensional Ising model (i.e., spins on a line)? In fact in one dimension, the Ising model can be solved exactly. It turns out that the system is paramagnetic for all  $T > 0$ , so there is no phase transition at any finite temperature. To see this, consider the ground state of the system in zero external field. This will have all spins aligned the same way (say up), and hence be ferromagnetic. Now consider a configuration with a various “domain walls” dividing spin up and spin down regions:

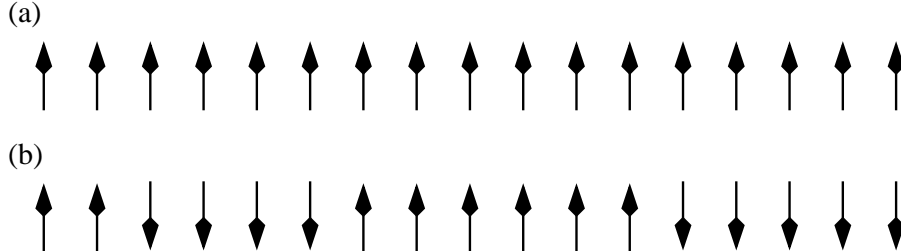


Figure 5: **(a)** Schematic of an Ising chain at  $T = 0$ . **(b)** At a small finite temperature the chain is split into domains of spins ordered in the same direction. Domains are separated by notional domain “walls”, which cost energy  $\Delta = 2J$ . Periodic boundary conditions are assumed.

Instead of considering the underlying spin configurations, let us first describe the system in terms of the statistics of its domain walls . The energy cost of a wall is  $\Delta = 2J$ , independent of position (prove it as an exercise!). Domain walls can occupy the bonds of the lattice, with  $N - 1$  bonds in an open-ended chain and  $N$  bonds in a periodic chain. Moreover, the walls are noninteracting, except that you cannot have two of them on the same bond. The total energy in the presence of  $n = 0, 1, \dots, N$  domain walls is given by  $E_n = -N J + n \Delta$ . In this representation, the partition function involves a count over all possible domain wall arrangements. Following the binomial statistics, there are  $W_n = \binom{N}{n} = N! / n!(N - n)!$  different configurations with  $n$  domain wall (and thus with energy  $E_n$ ) in a periodic chain with  $N$  bonds. Therefore, the partition function reads <sup>2</sup>

$$Z_N = \sum_{\{E_n\}} e^{-\beta E_n} = \sum_{n=0}^N \binom{N}{n} e^{-\beta E_n} = e^{\beta N J} \sum_{n=0}^N \binom{N}{n} e^{-\beta n \Delta} = e^{\beta N J} (1 + e^{-\beta \Delta})^N = Z_1^N \quad (14)$$

With  $Z_1 = e^{\beta J} (1 + e^{-\beta \Delta})$  standing for the partition function of a single bond with  $E_0 = -J$  and without  $E_1 = -J + \Delta$  a domain wall, i.e.,  $Z_1 = e^{-\beta(-J)} + e^{-\beta(-J+\Delta)}$ . Therefore, we showed that one can calculate  $Z_N$  by considering the partition function associated with a single bond of having or not having a domain wall. Then the free energy per bond of the system is

$$f = \frac{F}{N} = -\frac{1}{\beta} \ln Z_1 = -J - k_B T \ln(1 + e^{-\beta \Delta}). \quad (15)$$

The first term on the RHS is simply the energy per spin of the ferromagnetic (ordered) phase, while the second term arises from the entropy of domain walls. Clearly for any finite temperature (ie. for  $\beta < \infty$ ), this second term is finite and negative. Hence the free energy will always be lowered by having a finite concentration of domain walls in the system. Since these domain walls disorder the system, leading to a zero average magnetisation, the 1D system is paramagnetic for all finite temperatures.

<sup>2</sup>Here  $\{E_n\}$  includes all  $W_n$  configuration with energy  $E_n$ . Moreover  $(1 + X)^N = \sum_{n=0}^N \binom{N}{n} X^n$ .

### 3.2.1 Transfer matrix method

Generally speaking one-dimensional systems lend themselves to a degree of analytic tractability not found in most higher dimensional models. Indeed for the case of a 1d assembly of  $N$  spins each having  $m$  discrete energy states, and in the presence of a magnetic field, it is possible to reduce the evaluation of the partition function to the calculation of the eigenvalues of a matrix—the so-called *transfer matrix*. To illustrate this method, consider the joint energy  $E(s_i, s_j)$  of a pair of neighbouring spins  $s_i$  and  $s_j$ . If it is assumed that the assembly has cyclic boundary conditions, then the partition function may be written (note the period condition of the chain.)

$$\begin{aligned}
Z_N &= \sum_{\{s\}} \exp(-\beta E(\{s\})) \\
&= \sum_{\{s\}} \exp(-\beta [E(s_1, s_2) + E(s_2, s_3) + \dots + E(s_N, s_1)]) \\
&= \sum_{\{s\}} \exp(-\beta E(s_1, s_2)) \exp(-\beta E(s_2, s_3)) \dots \exp(-\beta E(s_N, s_1)) \\
&= \sum_{\{s_1, s_2, \dots, s_N\}} V_{s_1 s_2} V_{s_2 s_3} \dots V_{s_{N-1} s_N} V_{s_N s_1}
\end{aligned} \tag{16}$$

where we define the *transfer matrix*  $\mathbf{V}$  as follows

$$V_{s_1 s_2} = \exp(-\beta E(s_1, s_2)), \tag{17}$$

in which <sup>3</sup>

$$E(s_i, s_j) = -J s_i s_j - H \frac{s_i + s_j}{2}. \tag{18}$$

You should see that the sum over the product of matrix elements picks up all the terms in the partition function and therefore Eq. (16) is an alternative way of writing the partition function. Using bra-ket notation of quantum mechanics and noting that  $V_{s_1 s_2} = \langle s_1 | \mathbf{V} | s_2 \rangle$  we can rewrite the partition function in terms of the trace of  $\mathbf{V}^N$ :

$$Z_N = \sum_{\{s_1, s_2, \dots, s_N\}} \langle s_1 | \mathbf{V} | s_2 \rangle \langle s_2 | \mathbf{V} | s_3 \rangle \dots \langle s_{N-1} | \mathbf{V} | s_N \rangle \langle s_N | \mathbf{V} | s_1 \rangle = \sum_{s_1} \langle s_1 | \mathbf{V}^N | s_1 \rangle = \text{Tr}[\mathbf{V}^N]. \tag{19}$$

Since trace operation is basis-independent, we can rotate  $\mathbf{V}^N$  by a unitary transformation and diagonalise it with eigenvalues  $\lambda_{\pm}^N$  and thus we obtain

$$Z_N = \lambda_+^N + \lambda_-^N. \tag{20}$$

For very large  $N$ , this expression simplifies further because the largest eigenvalue  $\lambda_+$  dominates the behaviour since  $(\lambda_-/\lambda_+)^N$  vanishes as  $N \rightarrow \infty$ . Consequently in the thermodynamic limit one may put  $Z_N = \lambda_+^N$  and the problem reduces to identifying the largest eigenvalue of the transfer matrix. Specializing to the case of the simple Ising model in the presence of an applied field  $H$ , the transfer matrix takes the form

$$\mathbf{V} = \begin{pmatrix} e^{\beta(J+H)} & e^{-\beta J} \\ e^{-\beta J} & e^{\beta(J-H)} \end{pmatrix} \tag{21}$$

---

<sup>3</sup>Use following factorizing:  $e^{-\beta E\{s\}} = \dots \times e^{\beta H s_0/2} e^{\beta J s_0 s_1} e^{\beta H s_1/2} \times e^{\beta H s_1/2} e^{\beta J s_1 s_2} e^{\beta H s_2/2} \times \dots$

This matrix has two eigenvalues which can be readily calculated in the usual fashion as the roots of the characteristic polynomial  $|\mathbf{V} - \lambda\mathbf{I}|$ . They are <sup>4</sup>

$$\lambda_{\pm} = e^{\beta J} \cosh(\beta H) \pm \sqrt{e^{2\beta J} \sinh^2 \beta H + e^{-2\beta J}}. \quad (22)$$

Noting that the larger eigenvalue is  $\lambda_+$ , the free energy per spin  $f = F/N = -(k_B T/N) \ln Z_N = -k_B T \ln \lambda_+$  is

$$f = -J - k_B T \ln \left[ \cosh(\beta H) + \sqrt{\sinh^2 \beta H + e^{-4\beta J}} \right]. \quad (23)$$

We can immediately observe that, at  $H = 0$ , this free energy density is identical to the one obtained earlier in Eq. (15) through the use of the domain wall argument. The first part represents the energy density, while the second part pertains to the entropy contribution to the free energy. One can obtain the spontaneous magnetisation as follows

$$m = - \left( \frac{\partial f}{\partial H} \right)_T = \frac{\sinh \beta H}{\sqrt{\sinh^2 \beta H + \exp(-4\beta J)}}. \quad (24)$$

Evidently, the magnetization vanishes for zero magnetic field for a non-zero temperature. The Ising model in 2D can also be solved exactly, as was done by Lars Onsager in 1940. The solution is extremely complicated and is regarded as one of the pinnacles of statistical mechanics. In 3D no exact solution is known.

## 4 Mean Field Theory

Of the wide variety of models of interest to the critical point theorist, the majority have shown themselves intractable to direct analytic (pen and paper) assault. In a very limited number of instances models have been solved exactly, yielding the phase coexistence parameters, critical exponents and the critical temperature. The inability to solve many models exactly often means that one must resort to approximations. One such approximation scheme is Mean Field Theory. Mean Field Theory simplifies the study of systems with many interacting components by replacing the effect of each component with an average field. This simplification facilitates a more manageable mathematical analysis, enabling the understanding of the collective behavior of the entire system with a large number of particles.

### 4.1 Mean field solution of the Ising model

The average value of spin is given by  $\langle s_i \rangle$  and thus by considering the fluctuation  $\delta s_i$  we can write

$$s_i = \langle s_i \rangle + \delta s_i. \quad (25)$$

Note that  $\delta s_i$  stands for how much spin is deviated from its average value at lattice point  $i$ . Therefore, the spin interaction is give by

$$s_i s_j = (\langle s_i \rangle + \delta s_i)(\langle s_j \rangle + \delta s_j) = \langle s_i \rangle \langle s_j \rangle + \langle s_i \rangle \delta s_j + \langle s_j \rangle \delta s_i + \delta s_i \delta s_j. \quad (26)$$

---

<sup>4</sup>Solving this eigenvalue problem is left as an exercise.

In the mean field approximation, we assume that we can ignore the term quadratic in fluctuations:  $\delta s_i \delta s_j = 0$ . Moreover, we recall that the average spin is the magnetic moment (order parameter)  $m = \langle s_i \rangle$ .<sup>5</sup> Therefore, one can show that (exercise!)

$$s_i s_j = (m + (s_i - m))(m + (s_j - m)) = m(s_i + s_j - m) + \text{neglected fluctuation.} \quad (27)$$

Therefore, the energy (Hamiltonian) in the mean field approximation reads

$$E_I^{\text{MF}} = -J \sum_{\langle ij \rangle} m(s_i + s_j - m) - H \sum_i s_i. \quad (28)$$

Considering that the  $\langle ij \rangle$  is over nearest neighbour ( $nn$ ) spins we have<sup>6</sup>

$$\sum_{\langle ij \rangle} s_i = \frac{q}{2} \sum_{i=1}^N s_i. \quad (29)$$

The factor  $1/2$  is used to prevent double counting in the sum  $\sum_{\langle ij \rangle}$ , making it a sum over pairs rather than individual sites. The summation over  $j$  runs over the nearest neighbours, which gives  $\sum_{j \in nn} = q$  with  $q = 2$  for 1D,  $q = 4$  in 2D square lattice, and  $q = 6$  in 3D cubic lattice. Finally, one can easily obtain the following mean field energy

$$E_I^{\text{MF}} = \frac{q J N m^2}{2} - \bar{H} \sum_i s_i = \sum_{i=1}^N \left\{ \frac{q J m^2}{2} - \bar{H} s_i \right\}. \quad (30)$$

Here, we define a renormalised (or effective) magnetic field  $\bar{H} = H + q J m$ . As observed, the mean field energy is expressed as the sum over non-interacting particles (spins). We can calculate the partition function for a given spin  $s_i$ , which can have two possible energies for  $s_i = 1$  and  $s_i = -1$ . Therefore, we have:

$$Z(s_i) = e^{-\beta [\bar{H} + \frac{q J m^2}{2}]} + e^{-\beta [-\bar{H} + \frac{q J m^2}{2}]} = 2e^{\frac{-\beta q J m^2}{2}} \cosh(\beta \bar{H}). \quad (31)$$

Now, since all spins are identical and are assumed non-interacting, the partition function of the whole system is simply

$$Z = [Z(s_i)]^N. \quad (32)$$

Thus we find for the free energy (using Eq. (8))

$$f = \frac{F}{N} = \frac{q J m^2}{2} - k_B T \ln(2 \cosh(\beta \bar{H})). \quad (33)$$

From which, the magnetisation follows (cf. Fig 3) as

$$m = - \left( \frac{\partial f}{\partial H} \right)_T = \tanh(\beta \bar{H}) = \tanh(\beta(H + q J m)). \quad (34)$$

To find  $m(H, T)$ , we must numerically solve Eq. (34) self consistently.

---

<sup>5</sup>This aligns with Eq. (13) as, in this mean-field approach,  $\langle s_i \rangle$  is independent of the lattice site index  $i$ .

<sup>6</sup>Use  $\sum_{\langle ij \rangle} s_i = \frac{1}{2} \left( s_1 (\sum_{j=1}^q 1) + (\sum_{j=1}^q 1) s_1 + s_2 (\sum_{j=1}^q 1) + (\sum_{j=1}^q 1) s_2 + \dots \right)$ .

#### 4.1.1 Order parameter scaling: zero H solution

In zero magnetic field ( $H = 0$ ), we have

$$m = \tanh\left(\frac{mT_c}{T}\right) \quad (35)$$

where  $T_c = qJ/k_B$  is the critical temperature at which  $m$  first goes to zero. We look for a solution where  $m$  is small ( $\ll 1$ ). Expanding the tanh function and replacing  $\beta = (k_B T)^{-1}$  yields

$$m = \frac{mT_c}{T} - \frac{1}{3} \left(\frac{mT_c}{T}\right)^3 + O(m^5). \quad (36)$$

Then  $m = 0$  is one solution. The other solution is given by

$$m^2 = 3 \left(\frac{T}{T_c}\right)^3 \left(\frac{T_c}{T} - 1\right) \quad (37)$$

Now, considering temperatures close to  $T_c$  to guarantee small  $m$ , and employing the reduced temperature  $t = (T - T_c)/T_c$ , one finds

$$m^2 \simeq -3t \quad (38)$$

Hence

$$\begin{aligned} m &= 0 \text{ for } T > T_c \text{ since otherwise } m \text{ imaginary} \\ m &= \pm\sqrt{-3t} \text{ for } T < T_c \text{ real} \end{aligned}$$

#### 4.1.2 Magnetic susceptibility scaling: small H solution

Linear response function is defined as follows

$$m = \chi H \quad (39)$$

where  $\chi$  is the isothermal magnetic susceptibility that is independent from  $H$ . In a finite, but small field we can make the expansion

$$m = \frac{mT_c}{T} - \frac{1}{3} \left(\frac{mT_c}{T}\right)^3 + \frac{H}{kT} \quad (40)$$

Consider now the isothermal magnetic susceptibility  $\chi$

$$\chi = \left(\frac{\partial m}{\partial H}\right)_T = \frac{T_c}{T} \chi - \left(\frac{T_c}{T}\right)^3 \chi m^2 + \frac{1}{k_B T}$$

Then, it simplifies

$$\chi \left[ 1 - \frac{T_c}{T} + \left(\frac{T_c}{T}\right)^3 m^2 \right] = \frac{1}{k_B T} \quad (41)$$

Hence near critical point  $T \rightarrow T_c$ , we find

$$\chi = \frac{1}{k_B T_c} \left( \frac{1}{t + m^2} \right) \quad (42)$$

Therefore, the magnetic susceptibility is singular (diverges) at the critical point (where  $t = 0$  and  $m = 0$ ) and exhibits power-law scalings in its proximity

$$\begin{aligned} \text{for } T > T_c \rightarrow m^2 = 0 \rightarrow \chi &= (k_B T_c t)^{-1}, \\ \text{for } T \leq T_c \rightarrow m^2 &= -3t \rightarrow \chi = (-2k_B T_c t)^{-1}. \end{aligned}$$

where one has to take the non-zero value for  $m$  below  $T_c$  to ensure the thermodynamic stability. The schematic behaviour of the Ising order parameter and susceptibility are shown in fig. 6.

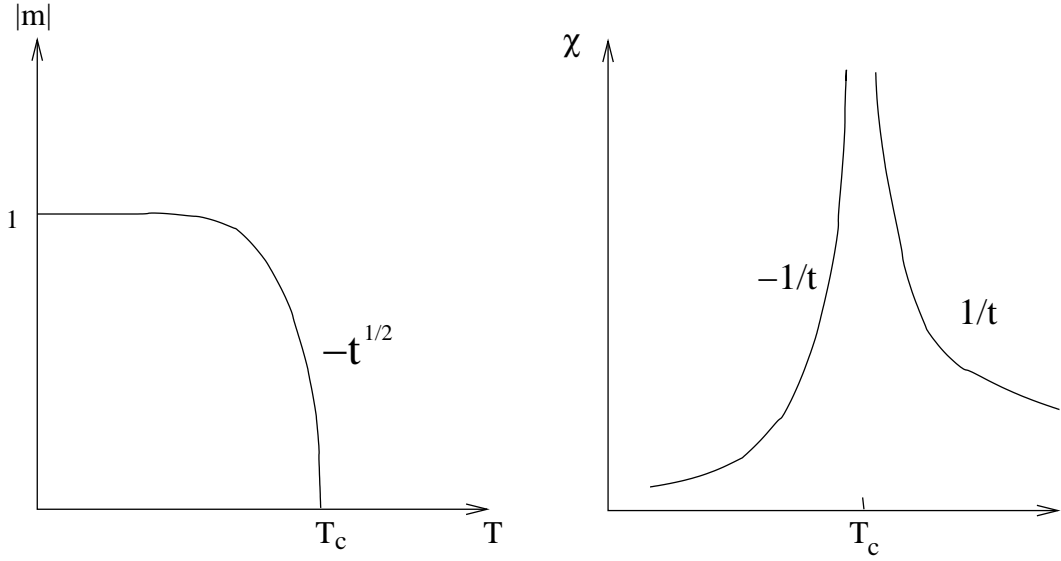


Figure 6: Mean field behaviour of the Ising magnetisation and susceptibility (schematic)

#### 4.1.3 Magnetisation scaling with magnetic field

Close to the critical point and for a small effective magnetic field, and assuming an infinitesimal external magnetic field  $H \ll Jqm$ , we can expand the self-consistent relation of the magnetisation as follows:

$$m \approx \beta_c \bar{H} - \frac{1}{3}(\beta_c \bar{H})^3 + \dots = m + \frac{H}{k_B T_c} - \frac{m^3}{3} + \dots \quad (43)$$

Therefore, we have the following scaling law close to the critical point in the mean field theory

$$m \propto H^{1/3}. \quad (44)$$

#### 4.1.4 Heat capacity scaling: zero $H$ solution

The heat capacity at constant  $H$  field is given by (exercise!)

$$C_H = -T \frac{\partial^2 F}{\partial T^2} \quad (45)$$

For  $H = 0$ , the mean field Free energy reads

$$\frac{F}{k_B T_c} = \frac{m^2}{2} - \frac{T}{T_c} \ln 2 - \frac{T}{T_c} \ln \left[ \cosh \left( \frac{m}{T/T_c} \right) \right] \quad (46)$$

Close to critical point we have  $m = \sqrt{3}|t|^{1/2}$  for  $T \leq T_c$  and  $m = 0$  for  $T > 0$ , and therefore we obtain (exercise! <sup>7</sup>)

$$F \approx \begin{cases} -k_B T \ln 2 + \dots & \text{if } T > T_c \\ -k_B T \ln 2 - \frac{3k_B T_c}{4}(1 - T/T_c)^2 + \dots & \text{if } T \leq T_c \end{cases} \quad (47)$$

Therefore, heat capacitance shows a discontinuous behaviour at the critical point

$$C_H \approx \begin{cases} 0 & \text{if } T > T_c \\ \frac{3k_B}{2} & \text{if } T \leq T_c \end{cases} \quad (48)$$

---

<sup>7</sup>Note  $\ln[\cosh(x)] \approx x^2/2 - x^4/12 + \dots$  for  $|x| \ll 1$ .

Therefore, the mean field theory predict that following scaling for the heat capacity

$$C_H \propto t^0. \quad (49)$$

#### 4.1.5 Correlation length scaling

The correlation length ( $\xi$ ) in the Ising model is a measure of the spatial extent over which spins in the system become correlated. It is related to the decay of spin correlations in the system. In the critical region, close to the critical temperature ( $T_c$ ), the correlation length diverges, indicating the presence of long-range correlations. The correlation length can be expressed in terms of the correlation function ( $G_{ij}$ ) as follows:

$$G_{ij} = \langle \delta s_i \delta s_j \rangle = \langle s_i s_j \rangle - \langle s_i \rangle \langle s_j \rangle \approx C(|\mathbf{r}_i - \mathbf{r}_j|) e^{-\frac{|\mathbf{r}_i - \mathbf{r}_j|}{\xi}} \quad (50)$$

where  $C(r)$  is a slow varying function and  $|\mathbf{r}_i - \mathbf{r}_j|$  is the distance between spins  $i$  and  $j$ . Near the critical point,  $\xi$  increases, signifying the emergence of large-scale correlations. This behaviour is a key feature of phase transitions in the Ising model. The mean field analysis reveals a power-law scaling behavior in the correlation length:

$$\xi \propto t^{-1/2}. \quad (51)$$

## 4.2 The Approach to Criticality

It is a matter of experimental fact that the approach to criticality in a given system is characterised by the divergence of various thermodynamic observables. Let us remain with the archetypal example of a critical system, the ferromagnet, whose critical temperature will be denoted as  $T_c$ . For temperatures close to  $T_c$ , the magnetic response functions (the magnetic susceptibility  $\chi$  and the specific heat) are found to be singular functions, diverging as a *power* of the reduced (dimensionless) temperature  $t \equiv (T - T_c)/T_c$ :

$$\chi \equiv \frac{\partial M}{\partial H} \propto t^{-\gamma} \quad (H = 0) \quad (52)$$

(where  $M = mN$ ),

$$C_H \equiv \frac{\partial E}{\partial T} \propto t^{-\alpha} \quad (H = \text{constant}) \quad (53)$$

Another key quantity is the correlation length  $\xi$ , which measures the distance over which fluctuations of the magnetic moments are correlated. This is observed to diverge near the critical point with an exponent  $\nu$ .

$$\xi \propto t^{-\nu} \quad (T > T_c, H = 0) \quad (54)$$

Similar power law behaviour is found for the order parameter  $m$  (in this case the magnetisation) which vanishes in a singular fashion (it has infinite gradient) as the critical point is approached as a function of temperature:

$$m \propto t^\beta \quad (T < T_c, H = 0), \quad (55)$$

(here the symbol  $\beta$ , is not to be confused with  $\beta = 1/k_B T$  – this unfortunately is the standard notation.) Finally, as a function of magnetic field:

$$m \propto h^{1/\delta} \quad (T = T_c, H > 0). \quad (56)$$

Table 1: Ising Model Exponents.

Exponents	$\alpha$	$\beta$	$\gamma$	$\delta$	$\nu$
Numerical ( $d = 3$ )	0.11	0.32	1.24	4.9	0.63
Exact ( $d = 2$ )	0	1/8	7/4	15	1
Mean field	0	1/2	1	3	1/2

with  $h = H/k_B T_c$ , the reduced magnetic field.

As examples, the behaviour of the magnetisation and correlation length are plotted in Fig. 7 as a function of  $t$ . **The quantities  $\alpha, \beta, \gamma, \delta, \nu$  in the above equations are known as critical exponents.** They serve to control the rate at which the various thermodynamic quantities change on the approach to criticality. Table 1 displays the values of these exponents for the Ising model, comparing mean field exponents to numerically estimated values in the three-dimensional case ( $d = 3$ ) and exact values obtained in the two-dimensional case ( $d = 2$ ) through Onsager's solution.

Remarkably, the form of singular behaviour observed at criticality for the example ferromagnet also occurs in qualitatively quite different systems such as the fluid (see the table in Fig. 7). All that is required to obtain the corresponding power law relationships for the fluid is to substitute the analogous thermodynamic quantities in to the above equations. Accordingly the magnetisation order parameter is replaced by the density difference  $\rho_{\text{liq}} - \rho_{\text{gas}}$  while the susceptibility is replaced by the isothermal compressibility and the specific heat capacity at constant field is replaced by the specific heat capacity at constant volume. The approach to criticality in a variety of qualitatively quite different systems can therefore be expressed in terms of a set of critical exponents describing the power law behaviour for that system.

Even more remarkable is the experimental observation that the values of the critical exponents for a whole range of fluids and magnets (and indeed many other systems with critical points) are *identical*. This is the phenomenon of *universality*. It implies a deep underlying physical similarity between ostensibly disparate critical systems. The principal aim of theories of critical point phenomena is to provide a sound theoretical basis for the existence of power law behaviour, the factors governing the observed values of critical exponents and the universality phenomenon. Ultimately this basis is provided by the Renormalisation Group (RG) theory, for which K.G. Wilson was awarded the Nobel Prize in Physics in 1982.

### 4.3 Spontaneous symmetry breaking and phase transition

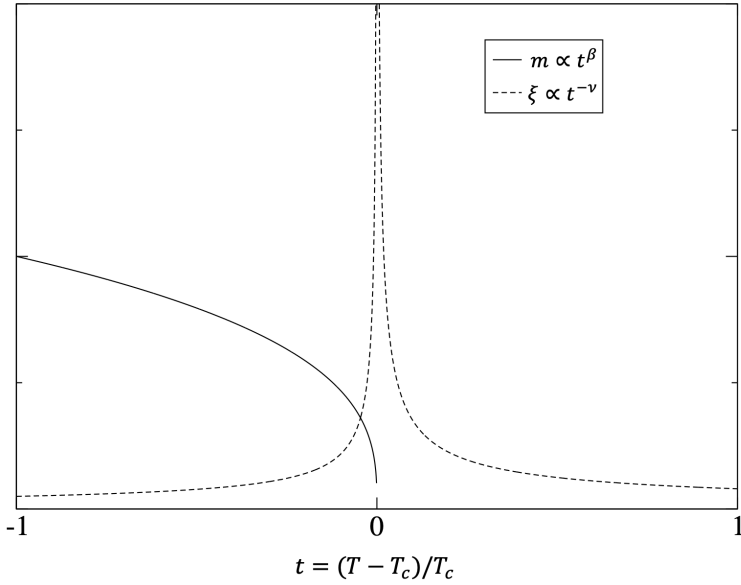
The mean field analysis reveals what is happening in the Ising model near the critical temperature  $T_c$ . In Fig. 8 you see sketches for  $\beta F(m)/N$  as a function of temperature, where for simplicity we restrict attention to  $H = 0$

In the absence of a field, the free energy function  $F(m)$  is symmetric in  $m$ . Moreover, at high  $T$ , the entropy dominates and there is a single minimum in  $F(m)$  at  $m = 0$ . At  $T$  is lowered, there comes a point ( $T = T_c$ ) where the curvature of  $F(m)$  at the origin changes sign; precisely at this point

$$\frac{\partial^2 F}{\partial m^2} = 0. \quad (57)$$

At lower temperature, there are instead two minima at nonzero  $m = \pm m^*$ , where the *equilibrium magnetisation*  $m^*$  is the positive root (calculated explicitly below) of

$$m^* = \tanh(\beta J q m^*) = \tanh\left(\frac{m^* T_c}{T}\right) \quad (58)$$



Transition type	Material	$\alpha$	$\beta$	$\gamma$	$\nu$
Ferromagnets ( $n = 3$ )	Fe, Ni	-0.1	0.4	1.3	
Superfluid ( $n = 2$ )	$\text{He}^4$	0	0.3	1.3	0.7
Liquid-gas ( $n = 1$ )	$\text{CO}_2$ , Xe	0.1	0.3	1.2	0.7
Ferroelectrics and superconductors	TGS	0	1/2	1	1/2
Mean-field theory		0	1/2	1	1/2

Figure 7: Top: Singular behaviour of the correlation length and order parameter in the vicinity of the critical point. Bottom: Critical exponents for specific heat ( $C \sim t^{-\alpha}$ ), order parameter ( $O \sim t^\beta$ ), susceptibility ( $\chi \sim t^{-\gamma}$ ), and correlation length ( $\xi \sim t^{-\nu}$ ) in different systems. [The table is taken from textbook *Statistical Physics of Fields* by Mehran Kardar.]

The point  $m = 0$  which remains a root of this equation, is clearly an unstable point for  $T < T_c$  (since  $F$  has a maximum there). This is an example of spontaneous symmetry breaking. In the absence of an external field, the configuration energy (and therefore the free energy) is symmetric under  $m \rightarrow -m$ . Accordingly, one might expect the actual state of the system to also show this symmetry. This is true at high temperature, but spontaneously breaks down at low temperature. Instead there are a pair of ferromagnetic states (spins mostly up, or spins mostly down) which – by symmetry – have the same free energy, lower than the unmagnetized state.

#### 4.3.1 Phase diagram: discontinuous (first-order) and continuous (second-order) transitions

The resulting zero-field magnetisation curve  $m(T, H = 0)$  looks like Fig. 9 (top panel). This shows the sudden change of behaviour at  $T_c$  (phase transition). For  $T < T_c$  it is arbitrary which of the two roots  $\pm m^*$  is chosen; typically it will be different in different parts of the sample (giving macroscopic “magnetic domains”). But this behaviour with temperature is *qualitatively modified* by the presence of a field  $H$ , however small. In that case, there is always a slight magnetization, even far above  $T_c$  and the curves becomes smoothed out, as shown.

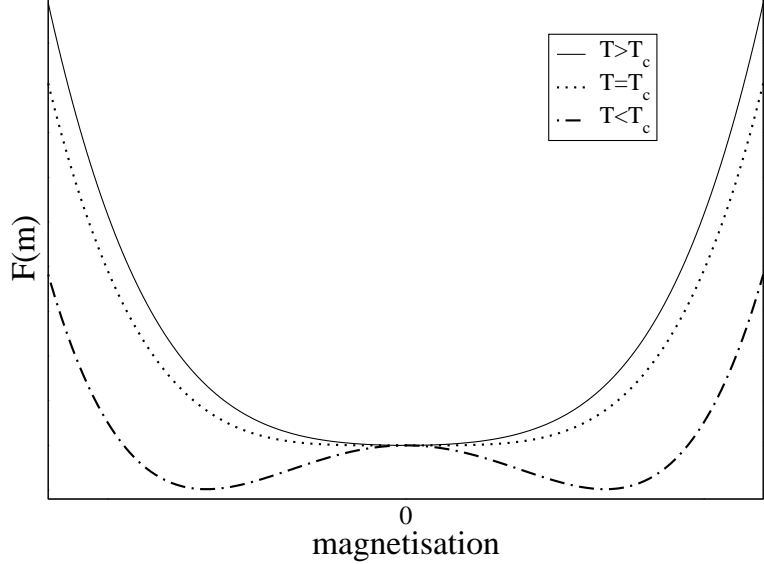


Figure 8: Schematic of the form of the free energy for a critical, sub-critical and supercritical temperature.

There is no doubt which root will be chosen, and no sudden change of the behaviour (no phase transition). Spontaneous symmetry breaking does not occur, because the symmetry is already broken by  $H$ . (The curve  $F(m)$  is lopsided, rather than symmetrical about  $m = 0$ .)

On the other hand, if we sit below  $T_c$  in a positive field (say) and gradually reduce  $H$  through zero so that it becomes negative, there is a *very* sudden change of behaviour at  $h = 0$ : the equilibrium state jumps discontinuously from  $m = m^*$  to  $m = -m^*$ . This is called a discontinuous phase transition as opposed to the continuous transition that occurs at  $T_c$  in zero field. The definitions are:

**Discontinuous transition:** magnetisation (or similar order parameter) depends discontinuously on a field variable (such as  $h$  or  $T$ ). This has been historically called a **first-order transition**. In this case, the phase transition is accompanied by the release of heat (latent heat), and all other thermodynamic quantities also experience discontinuity. Hysteresis behavior is also a characteristic of first-order transitions.

**Continuous transition:** Change of functional form, but no discontinuity in  $m$ ; typically, however,  $(\partial m / \partial T)_h$  (or similar) is either discontinuous, or diverges with an integrable singularity. This has been historically called a **second-order transition**. Critical power-law scaling, universality, and spontaneous symmetry breaking are relevant concepts for continuous transitions.

In this terminology, we can say that the phase diagram of the magnet in the  $H, T$  plane shows a line of discontinuous phase transitions, terminating at a continuous transition, which is the critical point.

## 5 Landau theory

Landau theory is a slightly more general type of mean field theory than that discussed in the previous subsection because it is not based on a particular microscopic model. Its starting point is the Helmholtz free energy, which Landau asserted can be written in terms of a truncated power series expansion of the order parameter. For a ferromagnet this takes the form

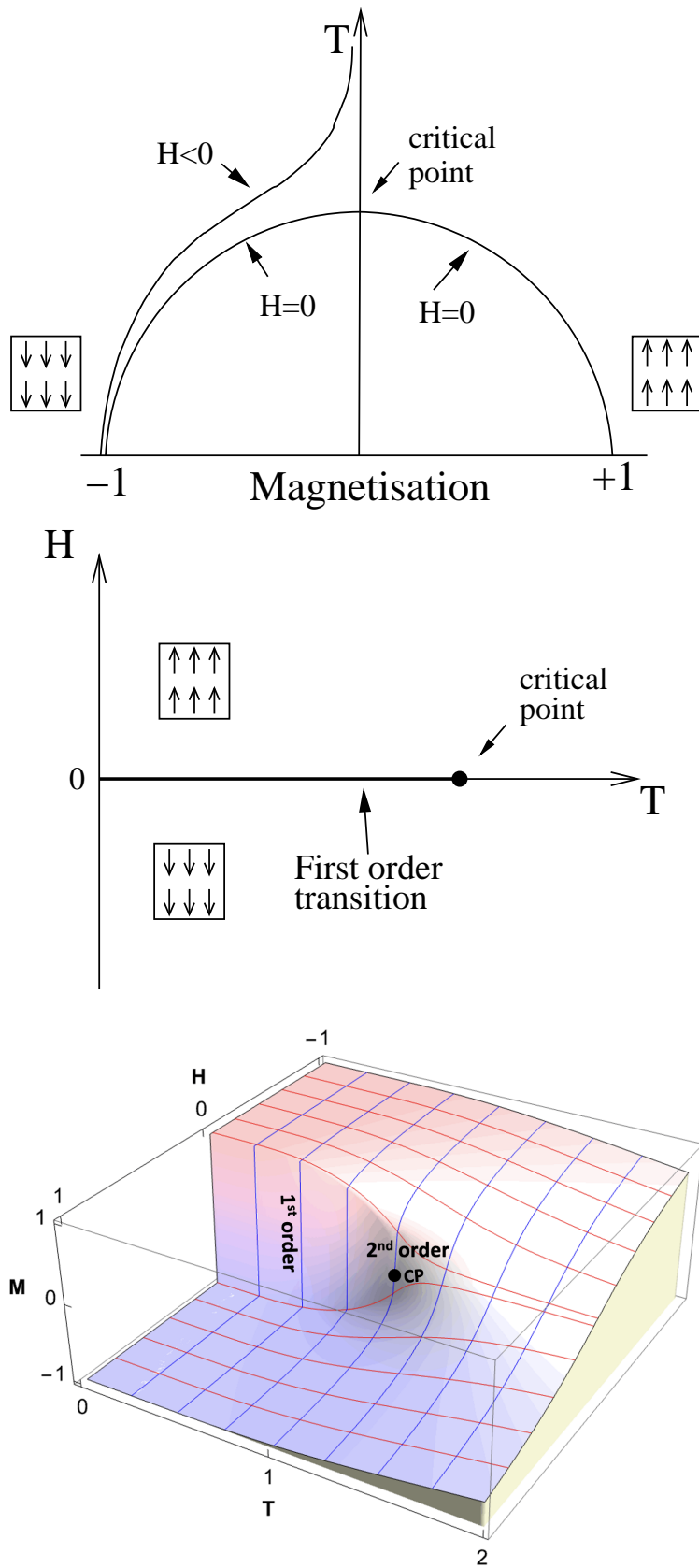


Figure 9: Top: Phase diagram of a simple magnet in the  $m - T$  plane. Middle: Phase diagram of a simple magnet in the  $H - T$  plane. Bottom: Mean field magnetization  $M$  in relation to temperature ( $T$  in the unit of  $T_c$ ) and magnetic field ( $H$  in the unit of  $k_B T_c$ ). The ferromagnetic critical point (CP) exhibits a discontinuous (first-order) transition below the critical temperature, while a continuous (second-order) phase transition occurs at  $T = T_c$ .

$$F(m) = F_0 + rm^2 + um^4 \quad (59)$$

( $F_0$  will be dropped from now on.)

Here only the terms compatible with the order parameter symmetry are included in the expansion. On symmetry grounds, the free energy of a ferromagnet should be invariant under a reversal of the sign of the magnetisation. Terms linear and cubic in  $m$  are not invariant under  $m \rightarrow -m$ , and so do not feature.

One can understand how the Landau free energy can give rise to a critical point by plotting its form for various values of  $r$  with  $u$  assumed positive (which ensures that the magnetisation remains bounded). The situation is qualitatively similar to that discussed in sec 4.3. Thermodynamics tells us that the system adopts the state of lowest free energy. For  $r > 0$ , the system will have  $m = 0$ , i.e. will be in the disordered (or paramagnetic) phase. For  $r < 0$ , the minimum in the free energy occurs at a finite value of  $m$ , indicating that the ordered (ferromagnetic) phase is the stable one. In fact, the physical (up-down) spin symmetry built into  $F$  indicates that there are two equivalent stable states at  $m = \pm m^*$ .  $r = 0$  corresponds to the critical point which marks the border between the ordered and disordered phases.

Clearly  $r$  controls the deviation from the critical temperature, and accordingly we may write

$$r = \tilde{r}t \quad (60)$$

where  $t$  is the reduced temperature. We can now attempt to calculate critical exponents. Restricting ourselves first to the magnetisation exponent  $\beta$  defined by  $m = |t|^\beta$ , we first find the equilibrium magnetisation, corresponding to the minimum of the Landau free energy:

$$\frac{dF}{dm} = 2\tilde{r}tm + 4um^3 = 0 \quad (61)$$

which implies

$$m \propto (-t)^{1/2}, \quad (62)$$

so  $\beta = 1/2$ , which is again a mean field result. Likewise we can calculate the effect of a small field  $H$  if we sit at the critical temperature  $T_c$ . Since  $r = 0$ , we have

$$F(m) = um^4 - Hm \quad (63)$$

then

$$\frac{\partial F}{\partial m} = 0 \Rightarrow m(H, T_c) = \left(\frac{H}{4u}\right)^{1/3} \quad (64)$$

or

$$H \sim m^\delta \quad \delta = 3 \quad (65)$$

which defines a second critical exponent. Note that at the critical point, a small applied field causes a very big increase in magnetisation; formally,  $(\partial m / \partial H)_T$  is infinite at  $T = T_c$ .

A third critical exponent can be defined from the magnetic susceptibility at zero field

$$\chi = \left(\frac{\partial m}{\partial H}\right)_{T,V} \sim |T - T_c|^{-\gamma} \quad (66)$$

*Exercise:* Show that the Landau expansion predicts  $\gamma = 1$ .

Finally we define a fourth critical exponent via the variation of the heat capacity (per site or per unit volume)  $C_H$ , in fixed external field  $H = 0$ :

$$C_H \sim |T - T_c|^{-\alpha} \quad (67)$$

By convention,  $\alpha$  is defined to be positive for systems where there is a *divergence* of the heat capacity at the critical point (very often the case). The heat capacity can be calculated from

$$C_H = -T \frac{\partial^2 F}{\partial T^2} \quad (68)$$

From the minimization over  $m$  (Eq. 61), one finds (*exercise*: check this)

$$\begin{aligned} F &= 0 & T > T_c \\ F &= -\frac{r^2}{4u} & T < T_c \end{aligned} \quad (69)$$

Using the fact that  $r$  varies linearly with  $T$ , we have

$$\begin{aligned} C_H &= 0 & T \rightarrow T_c^+ \\ C_H &= \frac{\tilde{r}^2}{2uT_c} & T \rightarrow T_c^- , \end{aligned} \quad (70)$$

which is actually a step discontinuity in specific heat. Since for positive  $\alpha$  the heat capacity is divergent, and for negative  $\alpha$  it is continuous, this behaviour formally corresponds to  $\alpha = 0$ .

## 5.1 Landau theory for $O(n)$ model

Consider a generalisation of the Ising model, in which the spins are not restricted to point along a single axis. In that case, the magnetisation is no longer the scalar  $m$ , but instead a vector  $\mathbf{m}$  with components  $m_i$ ,  $i = 1, \dots, n$ . Generally, the number of components for the magnetisation is independent of the spatial dimension of the system.

Although the magnetisation is a vector, a scalar order parameter can be defined,  $m = |\mathbf{m}|$ . Then, the Landau free-energy looks similar to the Ising model for any  $n$ :

$$\Delta F(m) = rm^2 + um^4 - \sum_i H_i m_i. \quad (71)$$

One difference is that the external field  $\mathbf{H}$  is also a vector, with components  $H_i$ .

## 5.2 Landau theory for nematic liquid crystals

In general, a liquid crystal is a fluid with some kind of orientational (but not full crystalline) order between the constituent molecules. Liquid crystals sit somewhere between fluids and crystalline solids. A nematic liquid crystal (from now on, simply a nematic) is the most common type, found in Liquid-Crystal Displays (LCDs). The order-disorder transition in three-dimensional nematics is an archetype of discontinuous phase transitions. It is much simpler to describe in mean-field theory than the liquid-to-crystal transition for freezing.

A crucial feature of a nematic is that the constituent molecules are not arrows like the magnetisation vector, but instead rods (or double-headed arrows). Therefore, a vector order parameter is not appropriate to describe a nematic liquid crystal. Instead, a rigorous description uses the symmetric traceless tensor (essentially just a matrix)  $Q_{ij} = S(n_i n_j - \delta_{ij}/3)$ . Here,  $n_i$  is a unit vector along the constituent molecules called the nematic director,  $\delta_{ij}$  is the Kronecker- $\delta$  (0 if  $i \neq j$ , 1 otherwise). Note that  $Q_{ij}$  does not change if  $n_i \rightarrow -n_i$ , reflecting the rod-like nature of

the fluid.  $S$  is the scalar order parameter, analogous to the absolute value of the magnetisation  $m$ . If  $S$  is zero, no nematic order is present, if  $S > 0$ , the fluid has nematic order. To get from the structure of  $Q_{ij}$  to a Landau free energy, we use the trace operator:  $\text{Tr}[A] = \sum_i A_{ii}$ . Note that  $\text{Tr}[Q] = 0$  by definition. However,  $\text{Tr}[Q^n]$  for some integer power  $n$  is nonzero, and is of order  $S^n$ . Therefore, we write the Landau free energy using  $\text{Tr}[Q^n]$  for  $n = 2, 3, 4$ , i.e., as a polynomial of  $S$ :

$$F(S) = rS^2 + wS^3 + uS^4. \quad (72)$$

Note the crucial difference with the Ising model and all of the O(N) models: the presence of the cubic term is  $wS^3$  in Eq. (72). This term is forbidden in O(N) models because the free energy has to have up-down symmetry  $m \rightarrow -m$ , i.e.,  $F$  cannot change sign under this operation. However,  $S \rightarrow -S$  does not correspond to any sort of up-down symmetry, and  $F(S)$  is allowed to have cubic terms (because in three dimensions,  $\text{Tr}Q_{ij}^3 \propto S^3$ ). Similarly, mean-field theories for solid-liquid transitions show a discontinuous behaviour due to the presence of cubic terms in the free energy.

## 6 Fluctuations and breakdown of mean-field theory

While mean field theories provide a useful route to understanding qualitatively the phenomenology of phase transitions, in real ferromagnets, as well as in more sophisticated theories, the critical exponents are not the simple fractions and integers found here. This failure of mean field theory to predict the correct exponents is of course traceable to their neglect of correlations. In later sections we shall start to take the first steps to including the effects of long-range correlations.

	Mean Field	$d = 1$	$d = 2$	$d = 3$
Critical temperature $k_B T/qJ$	1	0	0.5673	0.754
Order parameter exponent $\beta$	$\frac{1}{2}$	-	$\frac{1}{8}$	$0.325 \pm 0.001$
Susceptibility exponent $\gamma$	1	$\infty$	$\frac{7}{4}$	$1.24 \pm 0.001$
Correlation length exponent $\nu$	$\frac{1}{2}$	$\infty$	1	$0.63 \pm 0.001$

Table 2: Comparison of true Ising critical exponents with their mean field theory predictions in a number of dimensions.

### 6.1 Ginzburg criterion: when are fluctuations large?

Why does mean-field theory break down? In mean field theory, we assume negligible fluctuations. This, however, contradicts reality, where fluctuations and correlations are substantial when approaching the critical point. As mentioned before, the order parameter and Landau theory itself are defined in relation to a length scale, which is approximately on the order of correlation length  $\xi$ .

The breakdown of mean field theory and the effect of fluctuations can be discussed from different perspectives. A clue is that the spatial variations were ignored when constructing a Landau or mean-field theory. In a real material, the free energy will depend not only on the average magnetisation  $m$  but also its gradients  $\nabla m$ , i.e., the vector composed of spatial derivatives ( $\partial m / \partial x, \partial m / \partial y, \dots$ ). These gradient-dependent energies determine the importance of fluctuations: the bigger the energy cost for gradients, the more fluctuations are suppressed.

We can estimate these energy costs due to spatial variation of the magnetisation near a critical point by using **dimensional analysis** in combination with mean-field theory predictions. This gives rise to a self-consistency check on mean-field theory. Using an argument much like the one above to construct the Landau theory, we can estimate the free energy cost of gradients in  $m$ .

Intuitively, we can imagine that entropy favours the proliferation of gradients (because a system with varying  $m$  is more disordered) and we can make this intuition more precise. Since the energy is invariant under change of sign of  $m$ , the lowest-order gradient energy is proportional to  $\sum_i (\nabla m_i)^2$ , i.e.,  $(\partial m / \partial x)^2 + (\partial m / \partial y)^2 + \dots$ . To estimate the energy, we can use dimensional analysis. If the characteristic length scale of the system is  $\xi$ , then the square of the gradients will be of order  $\xi^{-2} m^2$  ( $m^2$  divided by length squared). To get the total energy, this energy *density* needs to be integrated over all space. This multiplies  $\xi^{-2} m^2$  by a factor of volume (for length scale  $\xi$ , this is  $\xi^d$ ). Therefore the total energy cost due to gradients will be of order  $\xi^{d-2} m^2$ . This is sometimes called the Ginzburg energy (or the Ginzburg term, see Advanced Topics for more details). Note that this expression applies for any dimensionality  $d = 1, 2, 3, \dots$  or any number of components  $N$  of the magnetisation (any  $O(N)$  model).

Now we assume that we are near the critical point and use the results of mean-field theory (here we assume that mean-field theory works, and find that in some case this leads to a contradiction).

Mean-field theory predicts  $m^2 \sim r/u \sim \xi^{-2}$  near the critical point, where the length scale  $\xi$  diverges as  $\xi \sim |t|^{-1/2}$ . Therefore, the Ginzburg energy term due to the spatial gradient of  $m$  scales as

$$\xi^{d-4}.$$

Because  $\xi \rightarrow \infty$  at the critical point, this term will suppress fluctuations and validate mean-field theory only for  $d > 4$ . In other words, achieving a gradient for  $m$  in dimensions  $d > 4$  demands a substantial energy cost. For precisely  $d = 4$ , the term still does not present a problem because it is just some lengthscale-independent number. However, for  $d < 4$ , fluctuations of the  $O(N)$  model are no longer regularised by the Ginzburg term, as gradients cost little energy near the critical point. Therefore the basic assumptions of mean-field theory break down for  $d < 4$ .

Note that for discontinuous transitions, the length scale divergence is cut off. Therefore, the Ginzburg term never vanishes (nor diverges) and this argument does not apply.

This Ginzburg criterion also shows that mean-field theory becomes exact for dimensionality  $d = 4$  and higher. This is why dimensional  $\epsilon$  expansion (where  $\epsilon = 4 - d$ ) is a good approach: it corrects mean-field theory away from this exact result.

## 7 The Static Scaling Hypothesis

The static scaling hypothesis is a plausible conjecture which is consistent with observed phenomena. Its basic assertion is that the singular dependence of the response functions enters through a single variable, namely the reduced temperature (or alternatively the correlation length  $\xi$ ) and that any other dependence on temperature is smooth and can be regarded as constant over a small temperature range around  $T_c$ .

The basis for scaling phenomena in near-critical systems is expressed in the claim that: in the neighbourhood of a critical point, the basic thermodynamic functions (most notably the Free energy) are *generalized homogeneous functions* of their variables. For such functions one can always deduce a scaling law such that by an appropriate change of scale, the dependence on two variables (e.g. the temperature and applied field) can be reduced to dependence on one new variable. This claim may be warranted by the following general argument.

A function of two variables  $g(u, v)$  is called a generalized homogeneous function if it has the property

$$g(b^{y_1}u, b^{y_2}v) = bg(u, v) \quad (73)$$

for all  $b$ , where the parameters  $y_1$  and  $y_2$  (known as scaling parameters) are constants. An example of such a function is  $g(u, v) = u^3 + v^2$  with  $y_1 = 1/3, y_2 = 1/2$ .

Now, the arbitrary scale factor  $b$  can be redefined without loss of generality as  $b^{y_1} = u^{-1}$  giving

$$g(u, v) = u^{1/y_1} g\left(1, \frac{v}{u^{y_2/y_1}}\right) \quad (74)$$

A corresponding relation is obtained by choosing the rescaling to be  $b^{y_2} = v^{-1}$ .

$$g(u, v) = v^{1/y_2} g\left(\frac{u}{v^{y_1/y_2}}, 1\right) \quad (75)$$

This equation demonstrates that  $g(u, v)$  indeed satisfies a simple power law in *one* variable, subject to the constraint that  $u/v^{y_1/y_2}$  is a constant. It should be stressed, however, that such a scaling relation specifies neither the function  $g$  nor the parameters  $y_1$  and  $y_2$ .

Now, the static scaling hypothesis asserts that in the critical region, the free energy  $F$  is a generalized homogeneous function of the (reduced) thermodynamic fields  $t = (T - T_c)/T_c$  and  $h = H/k_B T_C$ . For the ferromagnet, the following *ad hoc* scaling assumption can then be made:

$$F(b^{y_1}t, b^{y_2}h) = b^d F(t, h), \quad (76)$$

where  $b$  is a spatial rescaling factor (i.e., a ratio of length scales).

Without loss of generality, we can set  $b^{y_1} = t^{-1}$ , implying  $b = t^{-1/y_1}$  and  $b^{y_2} = t^{-y_2/y_1}$ .

Then

$$F(t, h) = t^{d/y_1} F(1, t^{-y_2/y_1}h) \quad (77)$$

where our choice of  $b$  ensures that  $F$  on the rhs is now a function of a single variable  $t^{-y_2/y_1}h$ .

Now, as stated in sec. 2 the free energy provides the route to all thermodynamic functions of interest. An expression for the magnetisation can be obtained simply by taking the derivative of free energy density  $f = F/N$  with respect to  $h$  (cf. Fig. 3):

$$\begin{aligned} m(t, h) &= -\left(\frac{\partial f}{\partial H}\right)_T \Big|_{H \rightarrow 0} = -\frac{1}{k_B T_C} \left(\frac{\partial f}{\partial h}\right)_T \Big|_{h \rightarrow 0} \\ &= t^{(d-y_2)/y_1} \left[ -\frac{1}{k_B T_C} \frac{\partial f(1, X)}{\partial X} \right]_{X(t^{-y_2/y_1}h) \rightarrow 0} = t^{(d-y_2)/y_1} m(1, t^{-y_2/y_1}h) \Big|_{h \rightarrow 0} \end{aligned} \quad (78)$$

In zero applied field  $h = 0$ , this reduces to

$$m(t, 0) = t^{(d-y_2)/y_1} m(1, 0) \quad (79)$$

where the r.h.s. is a power law in  $t$ . Equation (55) then allows identification of the exponent  $\beta$  in terms of the scaling parameters  $y_1$  and  $y_2$ .

$$\beta = \frac{d - y_2}{y_1}. \quad (80)$$

By taking further appropriate derivatives of the free energy, other relations between scaling parameters and critical exponents may be deduced. Such calculations yield the results<sup>8</sup>

$$\delta = y_2/(d - y_2), \quad (81)$$

$$\gamma = (2y_2 - d)/y_1, \quad (82)$$

$$\alpha = (2y_1 - d)/y_1. \quad (83)$$

Relationships between the critical exponents themselves can be obtained trivially by eliminating the scaling parameters from these equations. The principal results (known as “scaling laws”) are:

$$\alpha + \beta(\delta + 1) = 2 \quad (84)$$

$$\alpha + 2\beta + \gamma = 2 \quad (85)$$

Thus, provided all critical exponents can be expressed in terms of the scaling parameters  $y_1$  and  $y_2$ , then only two critical exponents need be specified, for all others to be deduced. Of course these scaling laws are also expected to hold for the appropriate thermodynamic functions of analogous systems such as the liquid-gas critical point.

## 7.1 Experimental Verification of Scaling

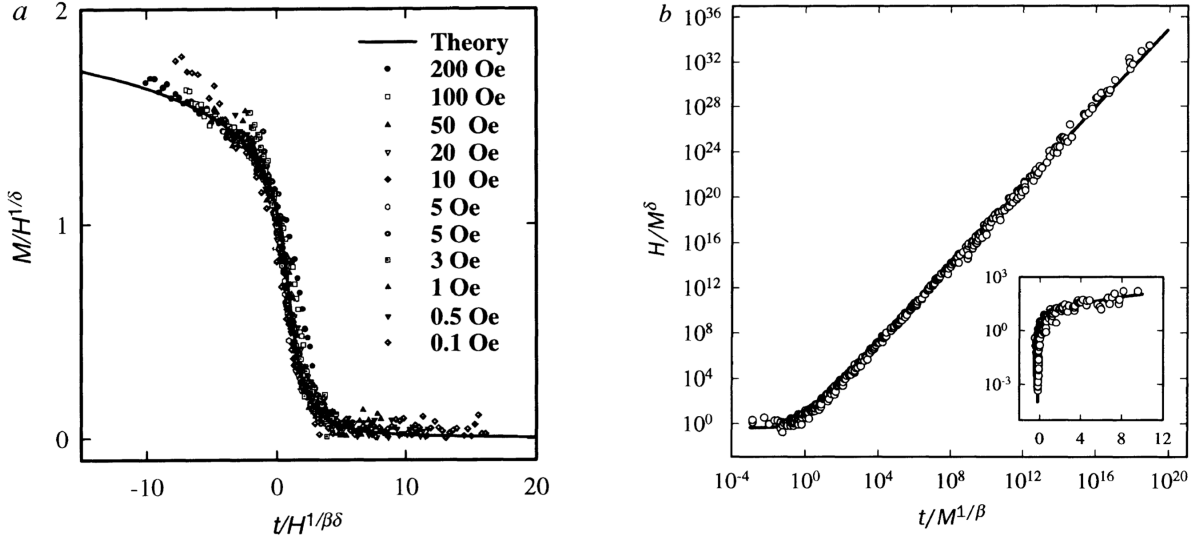


FIG. 4. *a*, Scaled magnetization  $M/H^{1/\delta}$  versus scaled temperature  $t/H^{1/\beta\delta}$  for the two films of Fig. 3. A linear scale is used. The solid line is the theoretical scaling function after ref. 6. For small fields, a discrete number of data points deviate from the scaling function. They are neglected in *b*. We used the value of  $\beta$  and  $\delta$  determined from Fig. 2. For  $\delta$  outside the range 12–16 the data collapsing is poorly realized.

This allows us to reduce the experimental uncertainty for  $\delta$  to  $\pm 2$ . *b*, Plot of  $H/M^\delta$  versus  $t/M^{1/\beta}$  for the two films of Fig. 3. The data with  $x > 0$  are represented as a log-log plot. The data points in the interval  $-1 < x < 10$  are represented semilogarithmically in the inset. The solid line is the theoretical curve from ref. 6. All data points, regardless of their value of  $H$ , are shown with the same symbol.

Figure 10: Experimental confirmation of universality for a phase transition in two dimensions was conducted on an atomic layer of ferromagnetic iron deposited on a non-magnetic substrate. The measured values of the exponents,  $\beta = 0.13 \pm 0.02$  and  $\delta = 14 \pm 5$ , closely align with the theoretical 2D Ising values, namely,  $\beta = 1/8 = 0.125$  and  $\delta = 15$  [C. H. Back et al., Nature 378, 597 (1995)].

The validity of the scaling hypothesis finds startling verification in experiment. To facilitate contact with experimental data for real systems, consider again Eq. (78). Eliminating the scaling parameters  $y_1$  and  $y_2$  in favour of the exponents  $\beta$  and  $\delta$  gives

---

<sup>8</sup>Exercise: try to derive these relationships

$$\frac{m(t, h)}{t^\beta} = m(1, h/t^{\beta\delta}) \quad (86)$$

where the RHS of this last equation can be regarded as a function of the single scaled variable  $\tilde{H} \equiv t^{-\beta\delta}h(t, M)$ . For some particular magnetic system, one can perform an experiment in which one measures  $m$  vs  $h$  for various fixed temperatures. This allows one to draw a set of isotherms, i.e.  $m - h$  curves of constant  $t$ . These can be used to demonstrate scaling by plotting the data against the scaling variables  $M = t^{-\beta}m(t, h)$  and  $\tilde{H} = t^{-\beta\delta}h(t, M)$ . Under this scale transformation, it is found that all isotherms (for  $t$  close to zero) coincide to within experimental error. This parametrisation is not the only possible way and for instance an experimental result is shown in Fig. 10 with different parametrisation which reads as follows (proving this scaling is left in an exercise.)

$$\frac{m(t, h)}{h^{1/\delta}} = m(t/h^{1/\beta\delta}, 1). \quad (87)$$

In summary, the static scaling hypothesis is remarkably successful in providing a foundation for the observation of power laws and scaling phenomena. However, it furnishes little or no guidance regarding the role of co-operative phenomena at the critical point. In particular it provides no means for calculating the values of the critical exponents appropriate to given model systems.

## 8 The Renormalisation Group Theory of Critical Phenomena

The critical region is characterised by correlated microstructure on *all* length-scales up to and including the correlation length. Such a profusion of degrees of freedom can only be accurately characterized by a very large number of variables. Mean-field theories and approximation schemes fail in the critical region because they at best incorporate interactions among only a few spins, while neglecting correlations over larger distances. The scaling hypothesis fails to provide more than a qualitative insight into the nature of criticality because it focuses on only one length-scale, namely the correlation length itself. Evidently a fuller understanding of the critical region may only be attained by taking account of the existence of structure on all length-scales. Such a scheme is provided by the renormalisation group method, which stands today as the cornerstone of the modern theory of critical phenomena.

### 8.1 The critical point: A many length scale problem

A near critical system can be characterized by three important length scales, namely

- (a) The correlation length,  $\xi$ , ie the size of correlated microstructure.
- (b) Minimum length scale  $L_{\min}$ , i.e. the smallest length in the microscopics of the problem, e.g. lattice spacing of a magnet or the particle size in a fluid.
- (c) Macroscopic size  $L_{\max}$  eg. size of the system.

The authentic critical region is defined by a window condition:

$$L_{\max} \gg \xi \gg L_{\min} \quad (88)$$

The physics of this regime is hard to tackle by analytic theory because it is characterized by configurational structure on all scales between  $L_{\min}$  and  $\xi$  (in fact it turns out that the near critical configurational patterns are *fractal*-like, cf. Fig. 3.1(b)). Moreover different length scales are correlated with one another, giving rise to a profusion of coupled variables in any theoretical description. The window regime is also not easily accessed by computer simulation because it entails studying very large system sizes  $L_{\max}$ , often requiring considerable computing resources.

## 8.2 Methodology of the RG (conceptual viewpoint)

The central idea of the renormalisation group (RG) method is a stepwise elimination of the degrees of freedom of the system on successively larger length-scales. To achieve this one introduces a fourth length scale  $L$ . In contrast to the other three, which characterize the system itself,  $L$  characterises the *description* of the system. It may be thought of as typifying the size of the smallest resolvable detail in a description of the system's microstructure.

Consider the Ising model arrangements displayed in Fig. 11. These pictures contain *all* the details of each configuration shown: the resolution length  $L$  in this case has its smallest possible value, coinciding with the lattice spacing i.e.  $L = L_{\min}$ . In the present context, the most detailed description is not the most useful: the essential signals with which we are concerned are hidden in a noise of relevant detail. A clue to eliminating this noise lies in the nature of the correlation length, i.e. the size of the largest droplets. The explicit form of the small scale microstructure is irrelevant to the behaviour of  $\xi$ . The small scale microstructure is the noise. To eliminate it, we simply select a larger value of the resolution length (or ‘coarse-graining’ length)  $L$ .

There are many ways of implementing this coarse-graining procedure. We adopt a simple strategy in which we divide our sample into blocks of side  $L$ , each of which contains  $L^d$  sites, with  $d$  the space dimensions . The centres of the blocks define a lattice of points indexed by  $I = 1, 2, \dots, N/L^d$ . We associate with each block lattice point centre,  $I$ , a coarse-grained or block variable  $S_I(L)$  defined as the spatial average of the local variables it contains:

$$S_I(L) = L^{-d} \sum_i^I s_i \quad (89)$$

where the sum extends over the  $L^d$  sites in the block  $I$ . The set of coarse grained coordinates  $\{S(L)\}$  are the basic ingredients of a picture of the system having spatial resolution of order  $L$ . The results of coarse-graining configurations typical of three different temperatures are shown in Fig. 11. Two auxiliary operations are implicit in these results. The first operation is a *length scaling*: the lattice spacing on each blocked lattice has been scaled to the same size as that of the original lattice, making possible the display of correspondingly larger portions of the physical system. The second operation is a *variable scaling*: loosely speaking, we have adjusted the scale (‘contrast’) of the block variable so as to match the spectrum of block variable values to the spectrum of shades at our disposal.

Consider first a system marginally above its critical point at a temperature  $T$  chosen so that the correlation length  $\xi$  is approximately 6 lattice spacing units. A typical arrangement (without coarse-graining, i.e.,  $L = 1$ ) is shown in Fig. 11(ai). The succeeding figures, 11(aii) and 11(aiii), show the result of coarse-graining with block sizes  $L = 4$  and  $L = 8$ , respectively. A clear trend is apparent. The coarse-graining *amplifies* the consequences of the small deviation of  $T$  from  $T_c$ . As  $L$  is increased, the ratio of the size of the largest configurational features ( $\xi$ ) to the size of the smallest ( $L$ ) is reduced. The ratio  $\xi/L$  provides a natural measure of how ‘critical’ is a configuration. The coarse-graining operation generates a representation of the system that becomes effectively less critical as the coarse-graining length increases. The limit

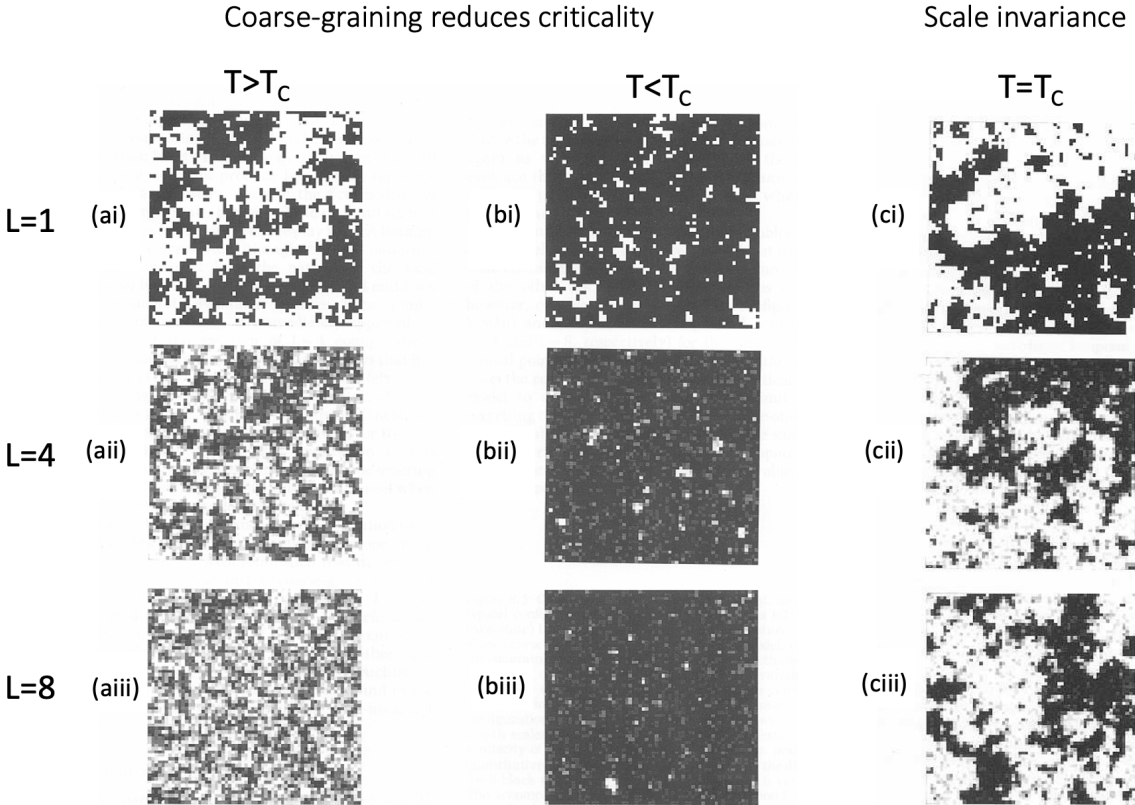


Figure 11: See text for details

point of this trend is the effectively fully disordered arrangement shown in Fig. 11(aiii). When the system is viewed on a scaled  $L$  larger than  $\xi$ , the correlated microstructure is no longer explicitly apparent; each coarse-grained variable is essentially independent of the others. A similar trend is apparent below the critical point. Fig. 11(bi) show a typical arrangement at a temperature  $T < T_c$  such that again  $\xi$  is approximately 6 lattice spacings. Coarse-graining with  $L = 4$  and  $L = 8$  again generates representations which are effectively less critical (Figs. 11(bii) and (bi)). This time the coarse-graining smoothes out the microstructure which makes the order incomplete.

Consider now the situation *at* the critical point. Fig. 11(ci) shows a typical arrangement; figs. 11(cii) and (ci) show the results of coarse-graining with  $L = 4$  and  $L = 8$  respectively. Since the correlation length is as large as the system itself the coarse graining does not produce less critical representations of the physical system: each of the figures displays structure over *all* length scales between the lower limit set by  $L$  and the upper limit set by the size of the display itself. A limiting trend is nevertheless apparent. Although the  $L = 4$  pattern is qualitatively quite different from the pattern of the local variables, the  $L = 4$  and  $L = 8$  patterns display qualitatively similar features. These similarities are more profound than is immediately apparent. A statistical analysis of the spectrum of  $L = 4$  configurations (generated as the local variables evolve in time) show that it is almost identical to that of the  $L = 8$  configurations (given the block variable scaling). The implication of this limiting behaviour is clear: the patterns formed by the ordering variable at criticality look the same (in a statistical sense) when viewed on all sufficiently large length scales.

Let us summarize. Under the coarse-graining operation there is an evolution or *flow* of the system's configuration spectrum. The flow tends to a limit, or fixed point, such that the pattern spectrum does not change under further coarse-graining. These scale-invariant limits have a

trivial character for  $T > T_c$ , (a perfectly disordered arrangement) and  $T < T_c$ , (a perfectly ordered arrangement). The hallmark of the critical point is the existence of a scale-invariant limit which is neither fully ordered nor fully disordered but which possesses structure on all length scales.

### 8.2.1 Fluid-magnet universality

Let us now turn to fluid-magnet universality. In a magnet, the relevant configurations are those formed by the coarse-grained magnetisation (the magnetic moment averaged over a block of side  $L$ ). In a fluid, the relevant configurations are those of the coarse-grained density (the mass averaged over a block of side  $L$ ) or more precisely, its fluctuation from its macroscopic average (Fig. 12). The patterns in the latter (bubbles of liquid or vapour) may be matched to pattern in the former (microdomains of the magnetisation), given appropriate scaling operations to camouflage the differences between the length scales and the differences between the variable scales. The results are illustrated in Fig. 13.

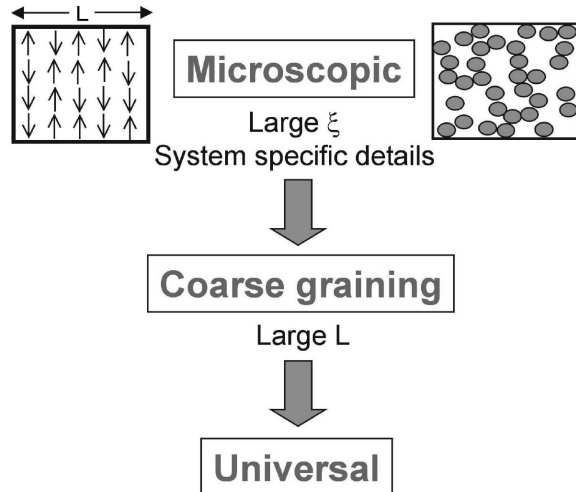


Figure 12: Schematic representation of the coarse graining operation via which the universal properties of fluids and magnets may be exposed.

### 8.2.2 Near critical scaling

The similarity of coarse-grained configurations of different systems is not restricted to the critical temperature itself. Suppose we have a two-state spin model and a three-state spin model each somewhat above their critical points at reduced temperature  $t$ . The two systems will have somewhat different correlation lengths,  $\xi_1$  and  $\xi_2$  say. Suppose, however, that we choose coarse grain lengths  $L_1$  for  $L_2$  for the two models such that  $\xi_1/L_1 = \xi_2/L_2$ . We adjust the scales of the block variables (our gray-level control) so that the typical variable value is the same for the two systems. We adjust the length scale of the systems (stretch or shrink our snapshots) so that the sizes of the minimum-length-scale structure (set by  $L_1$  and  $L_2$ ) looks the same for each system. Precisely what they look like depends upon our choice of  $\xi/L$ .

### 8.2.3 Universality classes

Coarse graining does not erase all differences between the physical properties of critical systems. Differences in the space dimension  $d$  of two critical systems will lead to different universal

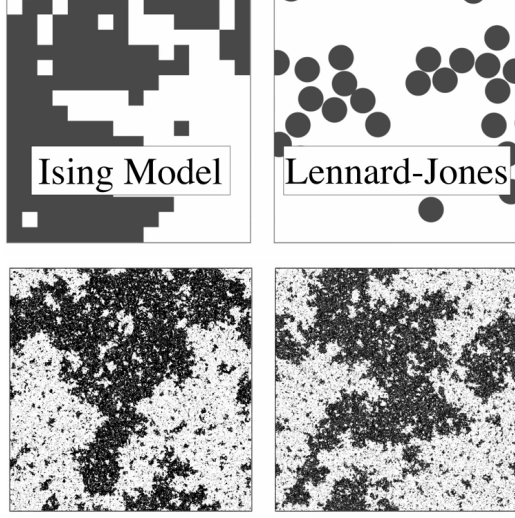


Figure 13: Snapshot configurations of the 2D critical Ising model (left) and the 2D critical Lennard-Jones fluid (right). When viewed on sufficiently large length scales the configurational patterns appear universal and self similar.

properties such as critical indices. Thus, for instance, the critical exponents of the 2D magnet match those of the 2d fluid, but they are different to those of 3d magnets and fluids.

In fact, the space dimension is one of a small set of qualitative features of a critical system which are sufficiently deep-seated to survive coarse graining and which together serve to define the system's universal behavior, or *universality class*. The constituents of this set are not all identifiable *a priori*. They include the number of components  $N$  of the order parameter in the  $O(N)$  model.

A third important feature that can change the universality class of a critical system is the range of the interaction potential between its constituent particles. Clearly for the Ising model, interactions between spins are inherently nearest neighbour in character. Most fluids interact via dispersion forces (such as the Lennard-Jones potential), which is also short-ranged due to the  $r^{-6}$  attractive interaction. However, some systems have much longer ranged interactions. Notable here are systems of charged particles that interact via a Coulomb potential. The long range nature of the Coulomb potential (which decays like  $r^{-1}$ ) means that charged systems often do not have the same critical exponents as the Ising model and fluid.

### 8.3 Continuous scaling: $\beta$ -function

It is intuitive to start thinking about renormalization as a discrete transformation, for example by mapping to a system with 2 times fewer degrees of freedom (spins) in each dimension. This would suggest that the length scaling factor  $b$  is an integer. However, we have already seen in the scaling hypothesis that it is convenient to consider  $b$  to be a general positive real number. To do so, we can consider comparing two strongly coarse-grained systems. Note that we can easily rescale, for example, by a factor of 2 or 3. Then, consider the Ising model with  $b = 8$  (coarse-grained by  $b = 2$  over and over 3 times,  $8 = 2^3$ ). Compare that with rescaling by  $b = 9$  (coarse-grained by a factor of  $b = 3$  just twice,  $9 = 3^2$ ). These two coarse-grained models have a relative scaling factor  $b = 9/8$ , and  $b$  can be taken arbitrarily close to  $b = 1$  by considering larger and larger fractions.

Thinking about the scaling factor  $b$  as a continuous variable allows us to consider the renormalization group *flow*. The flow is a set of differential equations that tell us how the parameters

of a model change under (an arbitrarily small) rescaling. By solving these equations, we get a picture of any rescaling, not just  $b \approx 1$ . For convenience, we will examine the change in thermodynamic quantities due to a change in  $\ln b$ . The logarithm means that if  $b = 1$ , which corresponds to no scaling, there is no change, and  $\ln b$  can be thought of the number of times that the system has been rescaled (by some factor, for example  $e$ ). Consider the Landau free energy  $F = rm^2 + um^4$  at two different length  $L$  and  $L'$  with scaling  $b = L'/L$  where  $b > 1$ ,

$$F(L) = r(L)m^2 + u(L)m^4, \quad (90)$$

$$F(L') = r(L')m^2 + u(L')m^4. \quad (91)$$

Since  $m$  is a control parameter that varies even for fixed  $L$ , we do not consider it as a function of rescaling. Therefore, we can obtain a dimensionless parameter that characterizes the *continuous* flow of the coupling parameter  $r$  under the rescaling process  $L' \rightarrow bL$  when  $b-1$  is infinitesimally small: <sup>9</sup>

$$\lim_{L' \rightarrow L} L \frac{r(L') - r(L)}{L' - L} = \lim_{b \rightarrow 1} \frac{r(bL) - r(L)}{b - 1} = L \frac{dr(L)}{dL} = \frac{dr(b)}{d \ln b} \quad (92)$$

and similarly for  $u(L)$ . We can then define so-called *beta functions*,

$$\beta_r = -\frac{dr(b)}{d \ln b}, \quad (93)$$

$$\beta_u = -\frac{du(b)}{d \ln b}. \quad (94)$$

We focus on these quantities because they let us characterize and compare different phase transitions and their universality classes. At a critical point (or in general at any fixed point), scale invariance dictates  $\beta$ -functions should vanish, i.e.,  $\beta_r = \beta_u = 0$ . A critical point is a fixed point of these differential equations. The high-temperature and low-temperature limits are other fixed points, and they are distinguished from the critical fixed point by how these equations behave near the fixed point.

To study the neighborhood of a fixed point, we expand the *beta function* around the fixed-point value in a Taylor series. For example, if  $r = 0$  is a critical point, then  $\beta(0) = 0$  and for a smooth function,  $\beta_r \approx -y_1 r + \dots$  Discarding the higher-order terms, we solve the differential equation near the critical point,

$$\frac{dr(b)}{d \ln b} = -\beta_r \approx y_1 r, \quad (95)$$

$$\rightarrow \frac{dr(b)}{r} = d \ln r(b) = y_1 d \ln b \rightarrow d(\ln r(b) - y_1 \ln b) = 0 \rightarrow r = r_0 b^{y_1}. \quad (96)$$

with  $r_0$  being the constant of the integration. This gives us critical exponents in terms of the Taylor coefficients of the beta function. For example, the lengthscale critical exponent  $\nu$  can be obtained by noting that any length, including the correlation length  $\xi$ , scales as  $\xi/b$ . (Note that when we coarse-grain and then rescale back to map onto the original model, then the correlation length decreases). On the other hand,  $r = \tilde{r}t$  scales as the rescaled temperature. So  $r \sim b^{y_1}$  implies that  $t \sim \xi^{-y_1}$  or  $\xi \sim |t|^{-1/y_1}$ . Comparing with the definition of the critical exponent  $\nu$ ,  $\xi \sim |t|^{-\nu}$  we conclude that  $\nu = 1/y_1$ . As we have seen from the static scaling hypothesis, we only need two independent exponents to find every other exponent. The beta functions  $\beta_r$  and  $\beta_u$  let us completely characterise the critical point of the Ising model (and any  $O(N)$  model).

---

<sup>9</sup>Note that  $b = e^\ell$ , where  $\ell = \ln b$  is the dimensionless scaling factor. For  $b \rightarrow 1$ , we have  $\ell \ll 1$ , so  $b \approx 1 + \ell + \dots$ , implying  $b-1 \approx \ell = \ln b$ . Moreover, for  $b \rightarrow 1$ , one can expand  $r(bL) = r(L) + L \partial_L r(L)(b-1) + \dots$

## 9 Methodology of the RG (effective coupling viewpoint)

Let us begin by returning to our fundamental equation, Eq. (4), which we rewrite as

$$p = Z^{-1} e^{-\mathcal{K}} \quad (97)$$

where  $\mathcal{K} \equiv E/k_B T$  is a rescaled configuration energy. The first step is then to imagine that we generate, by a computer simulation procedure for example, a sequence of configurations with relative probability  $\exp(-\mathcal{K})$ . We next adopt some coarse-graining procedure which produces from these original configurations a set of coarse-grained configurations. We then ask the question: what is the energy function  $\mathcal{K}'$  of the coarse-grained variables which would produce these coarse-grained configurations with the correct relative probability  $\exp(-\mathcal{K}')$ ? Clearly the form of  $\mathcal{K}'$  depends on the form of  $\mathcal{K}$  thus we can write symbolically

$$\mathcal{K}' = R\mathcal{K} \quad (98)$$

The operation  $R$ , which defines the coarse-grained configurational energy in terms of the microscopic configurational energy function is known as a renormalisation group transformation (RGT). What it does is to replace a hard problem by a less hard problem. Specifically, suppose that our system is near a critical point and that we wish to calculate its large-distance properties. If we address this task by utilizing the configurational energy and appealing to the basic machinery of statistical mechanics set out in eqs. 4 and 5, the problem is hard. It is hard because the system has fluctuations on all the (many) length scales intermediate between the correlation length  $\xi$  and the minimum length scale  $L_{\min}$ . However, the task may instead be addressed by tackling the statistical mechanics of the coarse-grained system described by the energy  $\mathcal{K}'$ . In order to provide a framework for a simple illustrative calculation, let us return to the lattice Ising model for which the energy function depended only on the product of nearest neighbour spins: <sup>10</sup>

$$\beta\mathcal{H} = -K \sum_{\langle ij \rangle} s_i s_j - h \sum_i s_i \quad (99)$$

where  $K = J/k_B T$  and  $h = H/k_B T$ . Since the original spins interact only with nearest neighbour spins and with the external field, we will make the courageous assumption that the block spins also interact only with nearest neighbour block spins and an effective external field. Our assumption implies that we should define new coupling constants between the block spins and an effective external field which interacts with the block spins. We will denote these respectively as  $K_b$  and  $h_b$ , with the subscript  $b$  reminding us that in principle, these coupling constants depend upon the definition of the block spins, and thence depend upon the coupling constants of the original Hamiltonian correspond to  $b = 1$ : thus, we have the boundary condition:  $K_1 = K$  and  $h_1 = h$ . The effective Hamiltonian  $H_b$  for the block spins is given by

$$\beta\mathcal{H}_b = -K_b \sum_{\langle IJ \rangle} \sigma_I \sigma_J - h_b \sum_I \sigma_I \quad (100)$$

Note that, in principle, the coarse-graining process has the potential to generate new terms in the Hamiltonian. However, for the moment, we disregard any new terms that may arise during the Renormalization Group (RG) process. The parameter  $b$  represents the number of iterations in the coarse-graining process, and the primary objective of RG is to ascertain how

---

<sup>10</sup>We note that it is not only useful to allow for arbitrary kinds of interactions: if we wish to repeat the transformation several (indeed many) times, it is also necessary because even if we start with only the nearest neighbour coupling in  $\mathcal{H}$  the transformation will in general produce others in  $\mathcal{H}'$ .

the coupling constants  $K_b$  and  $h_b$  evolve through successive RG transformations. The system described by  $\mathcal{H}_b$  is identical to that described by  $\mathcal{H}$ , except that the lattice spacing between the block spins is  $ba$ , while the spacing between the original spins is  $a$ . The former system also has fewer spins. Consequently, for the block spins, the correlation length measured in units of the spacing  $ba$  of the block spins, denoted as  $\xi_b$ , is smaller than the correlation length  $b$  of the initial system, measured in units of the spacing  $a$  between the original spins. This results in  $b\xi_b$  remaining unchanged, leading to

$$\xi_b = \xi/b. \quad (101)$$

This implies that the Hamiltonian resulting from the RG transformation has a smaller correlation length in the new unit, and the coarse-grained system is less critical. Since  $\xi_b = \xi/b < \xi$ , the coarse-grained system must be further from criticality than the original system. Thus, we conclude that it is at a new effective reduced temperature  $t \rightarrow t_b$  and reduced magnetic field  $h \rightarrow h_b$ .

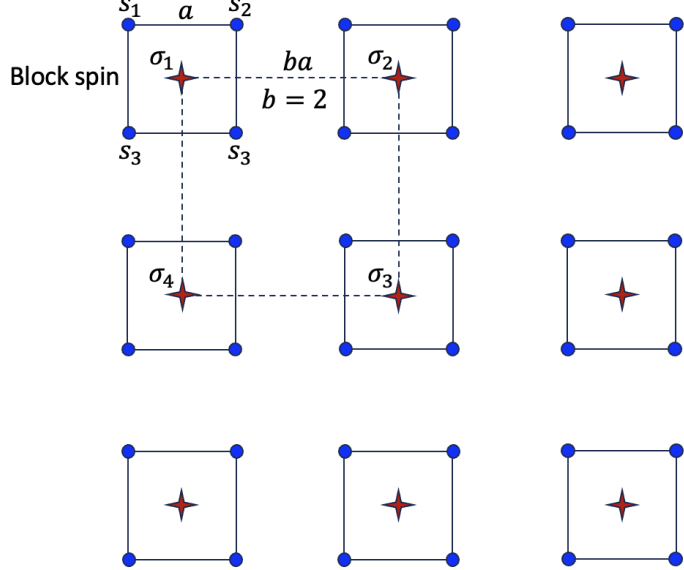


Figure 14: Coarse-graining process diagram. The blue circles indicate original spin and red stars show the block spin (coarse-grained spin). Parameter  $b$  is the rescaling length.

The effective Hamiltonian  $\mathcal{H}_b$  maintains the same structure as the original Hamiltonian, resulting in a free energy for the block spin system with the same functional form, substituting  $t_b$  and  $h_b$  for  $t$  and  $h$ . Therefore, we have  $F_b = N(ba)^{-d}f(t_b, h_b) = F = Na^{-d}f(t, h)$ <sup>11</sup> and thus

$$f(t, h) = b^{-d}f(t_b, h_b). \quad (102)$$

We still need to know how reduced temperature  $t_b$  transforms for block spin. To unravel power-law and scaling behaviour in the critical region, we assume that

$$t_b = tb^{y_t}, \quad h_b = hb^{y_h}. \quad (103)$$

---

<sup>11</sup>Here, one can also interpret that the number of degrees of freedom is reduced in the block spin RG procedure, where the initial spin number  $N$  is replaced by  $N' = N/b^d$ . For example, for  $d = 1$  and for a block consisting of two spins, with every RG transformation, we replace two spins  $s_1$  and  $s_2$  with one renormalized block spin  $\sigma_1$ . Therefore  $N \rightarrow N/2^1$ .

Assuming positive exponents  $y_t$  and  $y_h$ , we currently lack additional details. We substitute into free energy density to obtain

$$f(t, h) = b^{-d} f(tb^{y_t}, hb^{y_h}). \quad (104)$$

This is valid for arbitrary value of  $b$  and by setting  $b = |t|^{-1/y_t}$  we can prove the result of static scaling hypothesis as discussed in the earlier sections.

While the block spin transformation in the spin-half Ising model served as an example of such a transformation, we now contemplate a corresponding procedure for a general Hamiltonian  $\mathcal{H}$  resulting in an effective Hamiltonian for the long-wavelength degrees of freedom. We refer to this transformation as a renormalization group (RG) transformation which stands for the change or redefinition of coupling constants under a change of scale and a rescaling of degrees of freedom. Suppose that under  $R_b$ , the set of coupling constants become

$$[K'] \equiv R_b[K], \quad b > 1. \quad (105)$$

As before,  $R_b$  describes how the coupling constants change as the length scale, over which the local operators are defined, is varied. The transformations  $R_b$  for different  $b > 1$  do indeed form a semi-group: two successive transformations with  $b = b_1$  and  $b = b_2$  should be equivalent to a combined scale change of  $b_1 b_2$ :

$$[K'] \equiv R_{b_1}[K], \quad (106)$$

$$[K''] \equiv R_{b_2}[K'] = R_{b_2}R_{b_1}[K] = R_{b_1 b_2}[K]. \quad (107)$$

There are different RG method to calculate the transformation  $R_b$ . Lets write down the partition function of a system with  $N$  degree of freedom:

$$Z_N[K] = \text{Tr}[e^{-\beta\mathcal{H}}] = \sum_{\{s\}} e^{-\beta\mathcal{H}} \quad (108)$$

The free energy density then reads

$$f[K] = -\frac{1}{\beta N} \ln Z_N[K] \quad (109)$$

An RG transformation reduces the number of degrees of freedom by a factor  $b^d$ , leaving  $N' = N/b^d$  degrees of freedom, described by 'block variables'  $\{\sigma_I\}$ ,  $I = 1, \dots, N'$  with an effective Hamiltonian  $\mathcal{H}'_{N'}$ . Partially performing the trace on the spin degree of freedom, we obtain

$$e^{-\beta\mathcal{H}'\{\sigma\}} = \sum_{\{s\}} W(\{\sigma\}, \{s\}) e^{-\beta\mathcal{H}\{s\}} \quad (110)$$

where  $W(\{\sigma\}, \{s\})$  is a probability function (or projection operator) that is to perform an unrestricted trace. The projection operator reflect the symmetry of the system and must satisfy

$$W(\{\sigma\}, \{s\}) \geq 0 \quad \text{and} \quad \sum_{\{\sigma\}} W(\{\sigma\}, \{s\}) = 1. \quad (111)$$

So that the partition function for the new system is the same as before:

$$\begin{aligned} Z'_{N'} &= \sum_{\{\sigma\}} e^{-\beta\mathcal{H}'\{\sigma\}} = \sum_{\{\sigma\}} \sum_{\{s\}} W(\{\sigma\}, \{s\}) e^{-\beta\mathcal{H}\{s\}} = \sum_{\{s\}} \left[ \sum_{\{\sigma\}} W(\{\sigma\}, \{s\}) \right] e^{-\beta\mathcal{H}\{s\}} \\ &= \sum_{\{s\}} e^{-\beta\mathcal{H}\{s\}} = Z_N. \end{aligned} \quad (112)$$

This relation is valid up to a constant shift in the free energy, which can be generated during the Renormalization Group (RG) process. This shift has been neglected in the above relation. In one of the problems involving the 1D Ising model, we will explore an example of such a free energy shift in the RG transformation. Although the partition function remains the same under the RG transformation, the number of degrees of freedom is reduced by a factor of  $1/b^d$ . Therefore, the free energy transforms as follows:

$$f[K] = b^{-d} f[K']. \quad (113)$$

## 9.1 RG flows near a fixed point

In the RG method, the recognition of fixed points is crucial. If we know the RG transformation  $R_b[K]$ , a fixed point  $[K^*]$  in coupling constant space satisfies  $[K^*] = R_b[K^*]$ . In other words, fixed points are invariant under RGT. Under  $R_b$ , length scales are reduced by a factor  $b$ . For a specific set of coupling constants, the correlation length  $\xi$  transforms as  $\xi[K'] = \xi[K]/b$ , indicating a movement away from criticality. At a fixed point,  $\xi[K^*] = \xi[K^*]/b$ , implying  $\xi[K^*]$  can only be zero or infinity. We classify a fixed point with  $\xi[K^*] = \infty$  as a *critical fixed point* and a fixed point with  $\xi[K^*] = 0$  as a *trivial fixed point*. Generally, an RG transformation will have multiple fixed points, each with its own basin of attraction. Points within a basin of attraction flow toward and ultimately reach the fixed point after an infinite number of  $R_b$  iterations.

What insights can we gain from the behavior of flows near a fixed point? Let  $K_n = K_n^* + \delta K_n$ , indicating that the starting Hamiltonian is close to the fixed point Hamiltonian, i.e., the Hamiltonian with coupling constants equal to their fixed point values:  $\mathcal{H} = \mathcal{H}[K^*] = \mathcal{H}^*$ . Let  $\mathcal{H} = \mathcal{H}^* + \delta\mathcal{H}$ . Now, perform an RG transformation:  $[K'] = R_b[K]$ . The transformed coupling constants are given by

$$[K'] = [K^*] + [\delta K'], \quad (114)$$

where  $\delta K'_n$  is expressed by Taylor's expansion as

$$[K'] = [K^*] + \frac{\partial[K']}{\partial[K]} \Big|_{[K]=[K^*]} [\delta K] + \dots \quad (115)$$

Therefore,

$$[\delta K'] = M[\delta K] \rightarrow \delta K'_n = \sum_m M^{nm} \delta K_m \quad \text{where} \quad M^{nm} = \frac{\partial K'_n}{\partial K_m} \Big|_{K_m=K_m^*}. \quad (116)$$

Assuming a symmetric  $M_b^{nm}$  matrix, we can diagonalise it with eigenvalues  $\Lambda_b^{(a)}$  and eigenvector  $|\mathbf{e}^{(a)}\rangle$ . Group symmetry <sup>12</sup> implies  $\sum_{m'} M_b^{nm'} M_{b'}^{m'm} = M_{bb'}^{nm}$  and thus  $\Lambda_b^{(a)} \Lambda_{b'}^{(a)} = \Lambda_{bb'}^{(a)}$ . The later implies a power-low scaling for the eigenvalues of the the RG transformation matrix (exercise!):

$$\Lambda_b^{(a)} = b^{y_a} \quad (117)$$

with  $y_a$  being a number to be determined, but independent of  $b$ . In other words, we can write

$$y_a = \frac{\ln \Lambda_b^{(a)}}{\ln b}. \quad (118)$$

---

<sup>12</sup>In a precise mathematical sense, the RGT is not a Group because the RG process is irreversible.

We can write down the RG transformation relation along the principle axis  $|\mathbf{e}_b^{(a)}\rangle$  as  $\delta\mathbf{K} = \sum_a k^{(a)} |\mathbf{e}^{(a)}\rangle$  and thus

$$\delta\mathbf{K}' = \sum_a k^{(a)} \Lambda^{(a)} |\mathbf{e}^{(a)}\rangle. \quad (119)$$

Based on the value of  $\Lambda^{(a)}$ , we can identify three different possibilities

- **Relevant** directions:  $\Lambda^{(a)} > 1$  ( $y_a > 0$ ), coupling constant grows with increasing  $b$ .
- **Irrelevant** directions:  $\Lambda^{(a)} < 1$  ( $y_a < 0$ ), coupling constant shrinks with increasing  $b$ .
- **Marginal** directions:  $\Lambda^{(a)} = 1$  ( $y_a = 0$ ), coupling constant remains unchanged with increasing  $b$ .

## 9.2 RG flow diagram: schematic discussion

To illustrate this, consider the flow diagram for an Ising model with nearest neighbour coupling constant  $K_1 = J_1/k_B T$ , next nearest neighbour coupling constant  $K_2 = J_2/k_B T$  in an external field  $h = H/k_B T$ :

$$-\beta\mathcal{H} = K_1 \sum_{\langle ij \rangle} s_i s_j + K_2 \sum_{\langle\langle ij \rangle\rangle} s_i s_j + h \sum_i s_i \quad (120)$$

We assume that the RG transformation can new Hamiltonian in terms of the coarse-grained spin

$$-\beta\mathcal{H}' = K'_1 \sum_{\langle IJ \rangle} \sigma_I \sigma_J + K'_2 \sum_{\langle\langle IJ \rangle\rangle} \sigma_I \sigma_J + h' \sum_I \sigma_I \quad (121)$$

with a new lattice constant  $ba$  with  $b$  is the rescaling length. The flow diagram in the  $h = 0$  plane is shown in Fig. 9.2. We can identify three fixed point regime: (1) low-temperature fixed point where the coupling constant are very large ( $K_1 = \infty, K_2 = \infty$ ), (2) High temperature fixed point where the coupling constant are very small ( $K_1 = 0, K_2 = 0$ ) and system is effectively non-interacting, and (3) a critical flow line with a critical fixed point.

*Low-temperature fixed point:* At very low temperatures, all spins align in one direction, assuming they are all up spins. If we slightly increase the temperature, a few down spins may appear. However, the coarse-grained spins will still predominantly be up spins since the majority of spins in each block maintain an up orientation. Consequently, when we are near the low-temperature phase, the RG transformation will effectively map the system to an even lower-temperature phase. This fact is shown by the orientation of arrows on the flow diagram toward higher coupling values.

*High-temperature fixed point:* In the high-temperature regime, we observe small domains of up and down spins. As the temperature increases, the size of these domains decreases. Conversely, after performing the RG transformation, the coarse-grained lattice acquires a larger lattice constant, leading to a reduction in domain size in this new unit. Consequently, in the coarse-grained frame, we have smaller domains, indicating that the RG transformation shifts the system to a higher-temperature regime with smaller domain sizes. This aligns with what we previously mentioned about the change in correlation length under the RG transformation, i.e.,  $\xi' = \xi/b$ . This is illustrated by the orientation of arrows on the flow diagram toward lower coupling values.

By understanding the flow orientation at both low and high-temperature regimes and considering the continuity of the flow, we must have a flow line that separates the low-temperature region from the high-temperature region. It is possible to identify a *critical fixed point* on this line where the coupling constant does not change after applying the RG transformation. Let's label this fixed point by  $[K^*] = (K_1^*, K_2^*)$  and in order to understand the flow close to this fix point we consider a small deviation of the coupling constants from the fixed point:  $K_{1,2} = K_{1,2}^* + \Delta K_{1,2}$  and if we repeat another RG transformation we will get new value for the deviations as  $K_{1,2} = K_{1,2}^* + \Delta K'_{1,2}$  where the are related to the previous step via a two-by-two matrix transformation

$$\begin{pmatrix} \Delta K'_1 \\ \Delta K'_2 \end{pmatrix} = M_{2 \times 2} \begin{pmatrix} \Delta K_1 \\ \Delta K_2 \end{pmatrix}. \quad (122)$$

By diagonalizing the matrix  $M$ , we find two eigenvalues, denoted as  $\Lambda^{(1)}$  and  $\Lambda^{(2)}$ , which are perpendicular and along the critical line, respectively. The eigenvalue along the perpendicular direction to the critical line is relevant ( $\Lambda^{(1)} > 1$ ), indicating that the RG transformation will move the system away from the critical point. Conversely, the eigenvalue along the critical line is irrelevant ( $\Lambda^{(2)} < 1$ ), leading the system back toward the critical point. Through successive applications of the RG transformation, we can deduce a power-law scaling for the eigenvalues:  $\Lambda^{(i)} = b^{y_i}$ , where  $y_1 > 0$  and  $y_2 < 0$  to satisfy  $\Lambda^{(1)} > 1$  and  $\Lambda^{(2)} < 1$ . Using the eigenvectors, we can parameterize any vector  $\mathbf{v}[K_1, K_2]$  in the phase space as:  $\mathbf{v}[K_1, K_2] \equiv \mathbf{v}[t, p] = t|\mathbf{e}_t\rangle + p|\mathbf{e}_p\rangle$  where  $|\mathbf{e}_{t,p}\rangle$  represents the corresponding eigenvector for two eigenvalues of  $M$ , e.g.  $M|\mathbf{e}_t\rangle = \Lambda_t|\mathbf{e}_t\rangle$  and  $M|\mathbf{e}_p\rangle = \Lambda_p|\mathbf{e}_p\rangle$  that means  $|\mathbf{e}_p\rangle$  is along the critical line, while  $|\mathbf{e}_t\rangle$  is along the other critical line from the high-T fixed point to the low-T fixed point. According to the flow orientation in Fig. 9.2, we can conclude that  $\Lambda_t > 1$  and  $\Lambda_p < 1$ . Therefore, we can switch from  $(K_1, K_2)$  frame to  $(t, p)$  representation of the coupling constants.

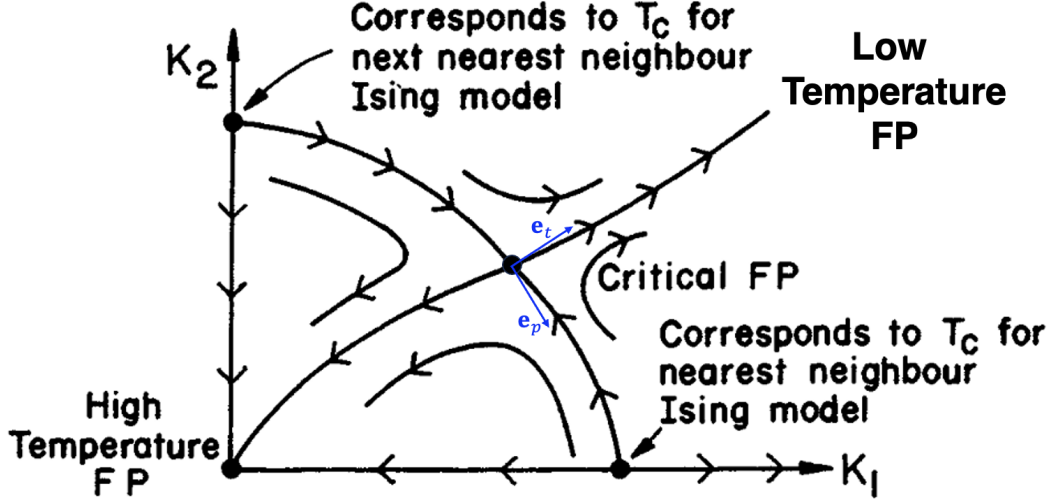


Figure 15: Schematic RG flow diagram of Ising mode with two coupling constant  $K_1$  and  $K_2$  standing for the nearest and next nearest neighbour interactions, respectively. [taken from N. Goldenfeld's lecture notes with a little change.]

Now, let's assume we apply the RG transformation  $n$  times over the vector  $\mathbf{v}$ . Therefore, we find

$$M^n \mathbf{v} = t^{(n)} |\mathbf{e}_t\rangle + p^{(n)} |\mathbf{e}_p\rangle \quad (123)$$

where  $t^{(n)} = t\Lambda_t^n = tb^{ny_t}$  and  $p^{(n)} = p\Lambda_p^n = pb^{ny_p}$ . Let's recall the rescaling of the correlation length after  $n$ -times RG transformation:  $\xi(K_1^{(n)}, K_2^{(n)}) = \xi(K_1, K_2)/b^n$ , where in the new basis it reads

$$\xi(t^{(n)}, p^{(n)}) = \xi(tb^{ny_t}, pb^{ny_p}) = \frac{\xi(t, p)}{b^n}. \quad (124)$$

Now, let's assume  $b = t^{-1/(ny_t)}$ , and therefore  $tb^{ny_t} = 1$ , leading to  $\xi(t, p) = t^{-1/y_t}\xi(1, pt^{-y_p/y_t})$ . Considering that  $y_p/y_t < 0$  and a small value of  $p \rightarrow 0$  close to the critical point, we obtain

$$\xi(t, p) = t^{-1/y_t}\xi(1, 0). \quad (125)$$

Assuming the parameter  $t$  as the reduced temperature  $t \sim |T - T_c|$ , we obtain a relation between the correlation length critical exponent and  $y_t$  as follows

$$\nu = \frac{1}{y_t}. \quad (126)$$

Although we have not computed the numerical value of  $\nu$  yet, we have drawn a clear relation between the critical exponent and the RG transformation matrix scaling behavior. Note that in the above definition,  $y_t$  is considered *relevant*, meaning it takes on positive real values ( $y_t > 0$  and thus  $\Lambda_t > 1$ ). As  $b$  becomes sufficiently large, the leading singularities of  $\xi$  are determined by relevant operators.

Concept	Key relation
Scaling parameter for $L \rightarrow L'$	$b = e^\ell = L'/L$
Correlation length rescaling	$\xi_b = \xi/b$
Beta-function at fixed point $[K^*]$	$\beta_r = -\frac{dr(b)}{d\ln b} _{[K]=[K^*]} = 0$
Free energy density as a homogeneous function	$f(t, h) = b^{-d}f'(tb^{y_t}, hb^{y_h})$
Linear RGT equation	$[\delta K'] = M[\delta K]$ and $M e_a\rangle = b^{y_a} e_a\rangle$
Relevant, Irrelevant, Marginal	$y_a > 0$ , $y_a < 0$ , $y_a = 0$
Correlation length exponent	$\xi \sim t^{-\nu}$ and $\nu = 1/y_t$ for $y_t > 0$

Table 3: Useful relations for RG transformation analysis.

### 9.3 RG analysis of 1D Ising model

Here, we implement RG method to 1D Ising model for practice the RG methodology for an exactly solvable system. The starting Hamiltonian is given by

$$-\beta\mathcal{H} = K \sum_i^N s_i s_{i+1} + h \sum_i^N s_i + \sum_i C \quad (127)$$

where  $K = J/k_B T$  and  $h = H/k_B T$ . We also include a constant term  $C$  which will be generated in the RG process even if it is zero in the original model. After RGT, the model is mapped to a new model with renormalized parameters

$$-\beta\mathcal{H}' = K' \sum_i^N s_i s_{i+1} + h' \sum_i^N s_i + \sum_i C' \quad (128)$$

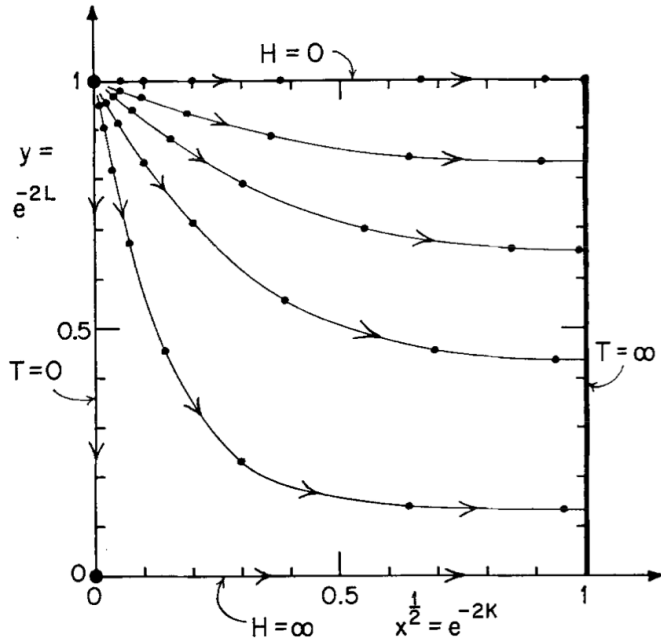


Figure 16: Flow diagram of 1D Ising model in the  $x$ - $y$  phase space is obtained by solving the recursive relations. Different curves corresponds to different starting points  $(x, y)$  shown in the plot legends. The flow line are from low temperature fixed point to high temperature fixed point and there is no critical fixed point with at finite critical temperature. [David R. Nelson, Michael E. Fisher, Annals Of Physics 91, 226-274 (1975).]

The RGT process leads to a set of recursive relations that relates old couplings to the new ones. We define new variables  $x = e^{-4K}$ ,  $y = e^{-2h}$ ,  $x' = e^{-4K'}$ ,  $y' = e^{-2h'}$ , and thus obtain the following recursion relations that can be solved to obtain the RG flow diagram [the derivation is straightforward but quite lengthy and it is left for a problem session discussion. Motivated reader can check David R. Nelson, Michael E. Fisher, Annals Of Physics 91, 226-274 (1975)].

$$x' = \frac{x(1+y)^2}{(1+xy)(x+y)}, \quad (129)$$

$$y' = \frac{y(x+y)}{1+xy}. \quad (130)$$

In the  $(x, y)$  parameter space, we obtain the fixed point by setting  $y' = y = y^*$  and  $x' = x = x^*$  leading to

$$x^* = \frac{x^*(1+y^*)^2}{(1+x^*y^*)(x+y^*)}, \quad (131)$$

$$y^* = \frac{y^*(x^*+y^*)}{1+x^*y^*}. \quad (132)$$

There are three fixed point solutions to these equations:

- $(x^*, y^*) = (0, 0)$ : High magnetic field regime with a frozen spin configuration fixed point
- $(x^*, y^*) = (0, 1)$ : Ferromagnetic fixed point with critical temperature  $T_c = 0$
- $(x^*, y^*) = (1, \text{arbitrary})$ : High temperature paramagnetic phase fixed point

The corresponding flow diagram is shown in Fig. 16. As seen (and expected in the 1D Ising model), the ferromagnetic fixed point at  $(x^*, y^*) = (0, 1)$  is unstable. Any RG transformation will move the system away from the fixed point and drive it toward the high-temperature paramagnetic phase, consistent with expectations in the 1D Ising model. The instability of the ferromagnetic fixed point can also be understood by examining the value of the linearized RG transformation matrix. By setting  $x' = x^* + \delta x'$  and  $x = x^* + \delta x$ , and similarly for  $y'$  and  $y$ , while keeping linearised terms, we find

$$\begin{pmatrix} \delta x' \\ \delta y' \end{pmatrix} = M \begin{pmatrix} \delta x \\ \delta y \end{pmatrix}, \quad M = \begin{pmatrix} 4 & 0 \\ 0 & 2 \end{pmatrix}. \quad (133)$$

Clearly, both eigenvalues of  $M$  are greater than 1. Consequently, both directions are *relevant*, leading the RG flow to move away from the fixed point, as illustrated by the arrows in the flow diagram in Fig. 16.

## 9.4 RG analysis of 2D Ising model: High-T expansion approach

This example illustrates how one can perform the renormalisation group transformation (98) directly, without recourse to a ‘sequence of typical configurations’. The calculation involves a very crude approximation which has the advantage that it simplifies the subsequent analysis.

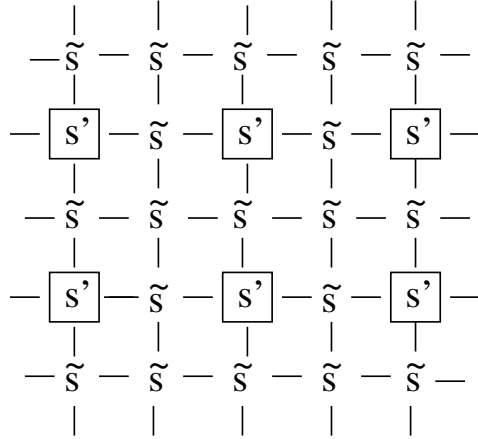


Figure 17: Coarse graining by decimation. The spins on the original lattice are divided into two sets  $\{s'\}$  and  $\{\tilde{s}\}$ . The  $\{s'\}$  spins occupy a lattice whose spacing is twice that of the original. The effective coupling interaction between the  $\{s'\}$  spins is obtained by performing the configurational average over the  $\{\tilde{s}\}$

Consider an Ising lattice model in two dimensions, with only nearest neighbour interactions as shown in Fig. 17. We have divided the spins into two sets, the spins  $\{s'\}$  form a square lattice of spacing 2, the others being denoted by  $\{\tilde{s}\}$ . One then defines an effective energy function  $\mathcal{H}'$  for the  $s'$  spins by performing an average over all the possible arrangements of the  $\tilde{s}$  spins

$$\exp(-\mathcal{H}') = \sum_{\{\tilde{s}\}} \exp(-\mathcal{H}). \quad (134)$$

This particular coarse-graining scheme is called ‘decimation’ because a certain fraction of spins on the lattice is eliminated. This formulation of a new energy function realizes two basic aims of the renormalisation group method: the long-distance physics of the ‘original’ system, described by  $\mathcal{H}$ , is contained in that of the ‘new’ system, described by  $R'$  (indeed the partition functions are the same) and the new system is further from criticality because the ratio of correlation

length to lattice spacing ('minimum length scale') has been reduced by a factor of  $1/2$  (the ratio of the lattice spacings of the two systems). We must now face the question of how to perform the configuration sum in Eq. (134). This cannot in general be done exactly, so we must resort to some approximation scheme. The particular approximation which we invoke is the high temperature series expansion. In its simplest mathematical form, since  $\mathcal{H}$  contains a factor  $1/k_B T$ , it involves the expansion of  $\exp(-\mathcal{H})$  as a power series:

$$\exp(-\mathcal{H}/k_B T) = 1 - \mathcal{H}/k_B T + \frac{1}{2!}(\mathcal{H}/k_B T)^2 + \dots \quad (135)$$

We substitute this expansion into the right hand side of Eq. (134) and proceed to look for terms which depend on the  $s'$  spins after the sum over the possible arrangements of the  $\tilde{s}$  spins is performed. This sum extends over all the possible ( $\pm 1$ ) values of all the  $\tilde{s}$  spins. The first term (the 1) in the expansion of the exponential is clearly independent of the values of the  $s'$  spins. The second term ( $\mathcal{H}$ ) is a function of the  $s'$  spins, but gives zero when the sum over the  $s'$  spins is performed because only a single factor of any  $s'$  ever appears, and  $+1 - 1 = 0$ . The third term ( $\mathcal{H}^2/2$ ) does contribute. If one writes out explicitly the form of  $\mathcal{H}^2/2$  one finds terms of the form  $K^2 s'_1 \tilde{s} s'_2 = K^2 s'_1 s'_2$ , where  $s'_1$  and  $s'_2$  denote two spins at nearest neighbour sites on the lattice of  $s'$  spins and  $\tilde{s}$  is the spin (in the other set) which lies between them. Now, in the corresponding expansion of the left hand side of Eq. (134), we find terms of the form  $K' s'_1 s'_2$ , where  $K'$  is the nearest neighbour coupling for the  $s'$  spins. We conclude (with a little more thought than we detail here) that

$$K' = K^2. \quad (136)$$

Of course many other terms and couplings are generated by the higher orders of the high temperature expansion. If our aim is to produce reliable values for the critical temperature and exponents it is necessary to include these terms. However, our aim here is to use this simple calculation to illustrate the renormalisation group method. Let us therefore close our eyes, forget about the higher order terms and show how the RGT (136) can be used to obtain information on the phase transition. The first point to note is that Eq. (136) has the fixed point  $K^* = 1$ ; if  $K = 1$  then the new effective coupling  $K'$  has the same value 1. Further, if  $K$  is just larger than 1, then  $K'$  is larger than  $K$ , i.e. further away from 1. Similarly, if  $K$  is less than 1,  $K'$  is less than  $K$ . We say that the fixed point is unstable: the flow of couplings under repeated iteration of Eq. (136) is away from the fixed point, as illustrated in fig. 18.

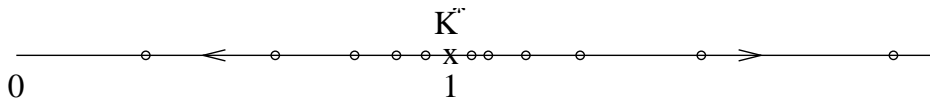


Figure 18: Coupling flow under the decimation transformation described in the text.

To expose the physical significance of these results let us suppose that the original system is at its critical point so that the ratio of correlation length to lattice spacing is infinite. After one application of the decimation transformation, the effective lattice spacing has increased by a factor of two, but this ratio remains infinite; the new system is therefore also at its critical point. Within the approximations inherent in Eq. (136), the original system is an Ising model with nearest neighbour coupling  $K$  and the new system is an Ising model with nearest neighbour coupling  $K'$ . If these two systems are going to be at a common critically, we must identify  $K' = K$ . The fixed point  $K^* = 1$  is therefore a candidate for the critical point  $K_c$ , where the phase transition occurs. This interpretation is reinforced by considering the case where the original system is close to, but not at, criticality. Then the correlation length is finite and the new system is further from critically because the ratio of correlation length to lattice spacing is reduced by a factor of two. This instability of a fixed point to deviations of  $K$  from  $K^*$  is a

further necessary condition for its interpretation as a critical point of the system. In summary then we make the prediction

$$K_c = J/k_B T_c = 1 \quad (137)$$

We can obtain further information about the behaviour of the system close to its critical point. In order to do so, we rewrite the transformation Eq. (136) in terms of the deviation of the coupling from its fixed point value. A Taylor expansion of the function  $K' = K^2$  yields

$$K' = K^* + (K - K^*) \left. \frac{\partial K'}{\partial K} \right|_{K=K^*} + \dots \rightarrow \Delta K' = 2\Delta K. \quad (138)$$

The deviation of the coupling from its fixed point (critical) value is thus bigger for the new system than it is for the old by a factor of two. This means that the reduced temperature is also bigger by a factor of two:

$$t' = 2t \quad (139)$$

But the correlation length (in units of the appropriate lattice spacing) is smaller by a factor of 1/2:

$$\xi' = \xi/2 \quad (140)$$

Thus, when we double  $t$ , we halve  $\xi$ , implying that

$$\xi \propto t^{-1} \quad (141)$$

for  $T$  close to  $T_c$ . Thus we see that the RGT predicts scaling behaviour with calculable critical exponents. In this simple calculation we estimate the critical exponent  $\nu = 1$  for the square lattice Ising model. This prediction is actually in agreement with the exactly established value. The agreement is fortuitous- the prediction in Eq. (137) for  $K_c$ , is larger than the exactly established value by a factor of more than two. In order to obtain reliable estimates more sophisticated and systematic methods must be used. The crude approximation in the calculation above produced a transformation, eq. 136, involving only the nearest neighbour coupling, with the subsequent advantages of simple algebra. We pay a penalty for this simplicity in two ways: the results obtained for critical properties are in rather poor agreement with accepted values, and we gain no insight into the origin of universality.

## 9.5 RG analysis of percolation

Here, we apply RGT to a critical phenomenon which is not, strictly, a thermodynamic phase transition. However, we will look at a simplified model for how a fluid goes through a porous solid, a phenomenon called *percolation*. The fluid could be hot water in a coffee percolator going through coffee grounds, or it could be water or petroleum going through porous rock or sand. This model has also been used in a more abstract sense to study communication in (eg online) networks or traffic on a city grid.

The model does not include temperature and considers the statistics of permanently placing bonds onto a square lattice (see Fig. 19). These bonds represent where the fluid has flowed through the pores. The probability that any bond is placed is  $p$ .  $p = 0$  corresponds to a totally empty lattice and  $p = 1$  corresponds to a completely occupied lattice. Consider two bonds separate by a distance  $r$ . We can ask deceptively simple questions about this model that do not have a simple answer. For example, what is the probability  $\mathcal{P}(r)$  that two occupied bonds distance  $r$  apart are connected to the same cluster (equivalently, that there is a path using occupied bonds that connects one of the these two bonds to the other)? At what occupation

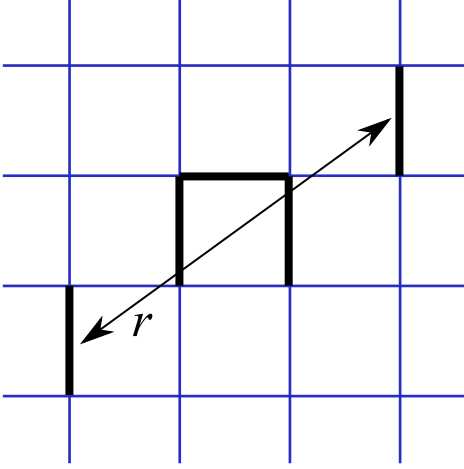


Figure 19: Percolation on a square lattice: black thick bonds are occupied, blue thin bonds are empty.

probability  $p = p_c$  is there a system spanning cluster (equivalently, that you can go from one side of an infinite lattice to the other side using occupied bonds)?

We can also reformulate this last question using  $\mathcal{P}(r)$ . Consider how to express  $\mathcal{P}(r)$  as a function of a dimensionless variable. We introduce a lengthscale  $\xi$ , which we will call the correlation length, by analogy. Then,  $r/\xi$  is a dimensionless variable, and we can assume that  $\mathcal{P}(r) = f(r/\xi)$  depends only on the ratio  $r/\xi$ . For  $p < p_c$ , there is a finite maximum cluster size so that  $\mathcal{P}(r) \rightarrow 0$  as  $r \rightarrow \infty$ . On the other hand, for  $p > p_c$ , the maximum cluster size is infinite and  $\mathcal{P}(r)$  goes to a finite value as  $r \rightarrow \infty$ . In between, the correlation length  $\xi$  must diverge as  $p$  approaches  $p_c$  from below. Therefore, we expect  $\xi \sim |p - p_c|^{-\nu}$  for some positive critical exponent  $\nu$ . We would like to (approximately) calculate  $p_c$  and  $\nu$  for this model.

We use a so-called real-space renormalization group approach, also called decimation. This involves mapping a 4-bond plaquette of the original lattice to a single diagonal bond of a new square lattice, rotated by  $45^\circ$  (see Fig. 20). This rescales each plaquette side by a factor of  $b = \sqrt{2}$ . Then, to compare with the original lattice, the new lattice is rotated and scaled down by a factor of  $b$ . The goal is to perform this decimation in such a way that preserves cluster connectivity and to map the probability  $p$  that any bond is occupied in the original lattice to the probability  $p'$  that a bond is occupied in the decimated lattice.

This mapping between  $p'$  and  $p$  can be performed in a graphical way (see Fig. 21):

$$p' = p^4 + 4p^3(1-p) + 2p^2(1-p)^2. \quad (142)$$

The terms on the right count the probabilities that a diagonal is connected in the original lattice. The first term,  $p^4$ , corresponds to a configuration where each of the four bonds of the plaquette is occupied. The second term,  $4p^3(1-p)$  considers the 4 different ways that three bonds are occupied (and one is unoccupied). The third term,  $2p^2(1-p)^2$  considers the two ways in which two bonds can be occupied (and two unoccupied) while connecting the diagonals. Note that no other configuration leaves the diagonal connected.

Equation (142) can be simplified to

$$p' = 2p^2 - p^4. \quad (143)$$

This relation allows us to estimate the critical probability  $p_c$ , map out the renormalization-group (RG) flow, and calculate the critical exponent  $\nu$ . First, let us find the fixed points  $p^* = p' = p$  for Eq. (143). At these points, the connectivity of the clusters does not change under this decimation procedure. At a fixed point,

$$(p^*)^4 - 2(p^*)^2 - p^* = 0 \quad (144)$$

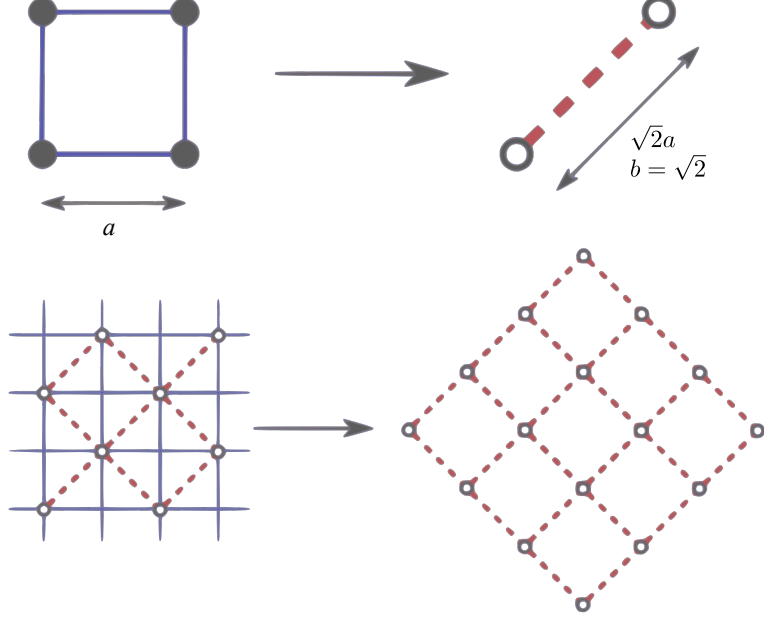


Figure 20: Set up for decimation for percolation on a square lattice. Each plaquette is mapped into a single bond.

or, factoring,

$$p^*(p^* - 1)[(p^*)^2 + p^* - 1] = 0. \quad (145)$$

The solution to this equation are the two trivial fixed points,  $p^* = 0$  and  $p^* = 1$  (corresponding to the empty and full phases, respectively) as well as the critical point

$$p_c = p^* = \frac{-1 + \sqrt{5}}{2} = \frac{1}{\phi} \approx 0.62 \quad (146)$$

which is the positive solution to  $(p^*)^2 + p^* - 1 = 0$  ( $\phi$  is the golden ratio!).

Now we can check that the RG flows away from the critical fixed point towards the trivial fixed points, and find the critical exponent  $\nu$ . We expand the right-hand side of the relation Eq. (143) in a Taylor series around  $p = p_c$ . Let us name  $\delta p' = p' - p_c$  and  $\delta p = p - p_c$ . Then, Eq. (143) becomes,

$$\delta p' + p_c = 2(\delta p + p_c)^2 - (\delta p + p_c)^4 = 2p_c^2 - p_c^4 + 4p_c\delta p - 4p_c^3\delta p + \dots \quad (147)$$

where we have kept terms only up to linear order in  $\delta p$ . When  $\delta p' = \delta p = 0$ , this Eq. (147) has to be satisfied by the definition of  $p_c$ , so all of the terms independent of  $\delta p'$  and  $\delta p$  cancel. The final expression is then

$$\delta p' = 4p_c(1 - p_c^2)\delta p, \quad (148)$$

which has the desired form  $\delta p' = \Lambda\delta p$ , with  $\Lambda = 4p_c(1 - p_c^2)$ . Indeed, since  $\Lambda > 1$  (it is relevant), we can see that the RG flow is away from the critical point  $p_c$  (see Fig. 22). Above the critical point,  $\delta p$  is positive and  $\delta p'$  is larger than  $\delta p$ . Below the critical point,  $\delta p$  is negative and  $\delta p'$  flows towards even smaller (more negative) values.

To calculate the critical exponent  $\nu$  from  $\Lambda$ , we go back to the definition of correlation length close to the critical point as  $\xi \sim |p - p_c|^{-\nu} = |\delta p|^{-\nu}$ . Under decimation,  $\xi \rightarrow \xi/b$  (with

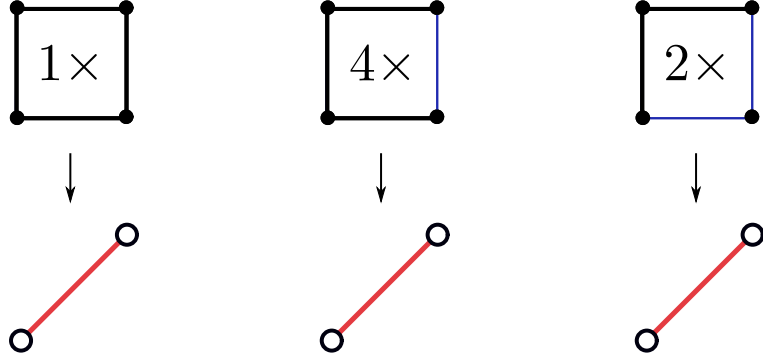


Figure 21: How to find the mapping between  $p'$  and  $p$ . There are three ways to keep the diagonal vertices connected: 4 bonds (left), 3 bonds (middle), and 2 bonds (right), with different probabilities and counting prefactors for each term.

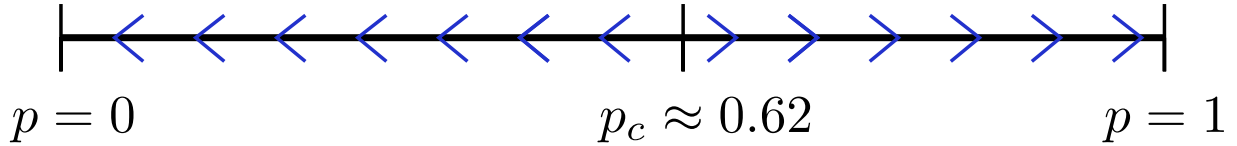


Figure 22: Renormalization group flow from decimation for percolation on a square lattice. There is one critical point  $p_c$  from which RG flows and two trivial fixed points  $p = 0$  and  $p = 1$  towards which RG flows.

$b = \sqrt{2}$ , since the lattice has to be scaled down to compare with the original one). Similarly,  $\delta p \rightarrow \delta p' = 4p_c(1 - p_c^2)\delta p$  where we have used the previously derived Eq. (148). Combining, we find that

$$\xi \sim |\delta p|^{-\nu} \rightarrow \xi/b \sim \Lambda^{-\nu} |\delta p|^{-\nu}. \quad (149)$$

This leaves  $\Lambda \sim b^{y=1/\nu}$  which we solve for  $\nu$  (see also equations (118) and (126)):

$$\nu = \frac{1}{y} = \frac{\ln b}{\ln \Lambda} = \frac{\ln \sqrt{2}}{\ln 4p_c(1 - p_c^2)} \approx 0.82 \quad (150)$$

where we have used  $b = \sqrt{2}$  and  $p_c = (-1 + \sqrt{5})/2$ . We have calculated a critical exponent using the renormalization group! We found it to be irrational, unlike the simpler mean-field exponents.

Although calculating the critical exponent  $\nu$  and making better approximations is difficult, there is a simple duality argument for the exact value of the critical probability  $p_c$  on a square lattice that lets us test the RG approach above. The argument relies on mapping the plaquettes (squares) of the original lattice to vertices of the new lattice and occupied bonds to empty bonds (and vice versa) of the new lattice. The bonds are mapped in this way: in the new lattice, a bond is occupied only if in the original lattice the bond (which is shared between these two plaquettes) is empty. This maps a lattice with occupation probability  $p$  to an identical lattice with occupation probability  $q = 1 - p$ . At the critical point, not only should  $p_c = q_c$  since they are the same model, but also  $q_c = 1 - p_c$  since a critical point in the original lattice should map to the critical point in the new lattice. The (unique) solution to these two equations is simple:  $p_c = q_c = 1/2$ . Recall that renormalization group predicts  $p_c = 0.62$ , which is not exactly right but also not too far off. However unlike critical exponents, the quantity  $p_c$  is not universal, which is not what we are after using the renormalization group approach.

# 10 Advanced topics (optional reading)

## 10.1 Landau-Ginzburg theory

In writing down a Landau free-energy density for the Ising model, we assumed that the free energy depends only on orientation of a single patch of spins at a point,

$$F(m(\mathbf{x})) = rm^2(\mathbf{x}) + um^4(\mathbf{x}), \quad (151)$$

where  $\mathbf{x}$  is the position vector. However, spatial variations in  $m(\mathbf{x})$  will also affect the free-energy density. This is easy to see in the Ising model, because the relative orientation of the neighboring spins do affect the free energy.

Therefore, we would like to incorporate the gradient  $\nabla m(\mathbf{x})$  into the free-energy expression. Note that the term  $\nabla m(\mathbf{x})$  by itself cannot enter the free energy both because it is a vector and because it is odd in  $m$ . However, the quadratic term  $\nabla m(\mathbf{x}) \cdot \nabla m(\mathbf{x})$  is suitable.

For the more general O(N) model, this term has the form

$$\sum_{ij} \nabla_i m_j(\mathbf{x}) \nabla_i m_j(\mathbf{x}). \quad (152)$$

Similarly, for the  $Q$ -tensor, the appropriate term is:

$$\sum_{ijk} \nabla_i Q_{jk}(\mathbf{x}) \nabla_i Q_{jk}(\mathbf{x}). \quad (153)$$

where the gradient indices and the order parameter vector/tensor indices do not mix. Again, this reflects that the order lives in orientation or spin-space, and not in physical space. In general, these two spaces can be different and have different dimensionalities.

## 10.2 Statistical field theory

There is a big conceptual leap when going from a Landau theory to a Landau-Ginzburg theory. In the Landau-Ginzburg theory, the quantity  $F(m(\mathbf{x}))$  depends on the spatial position  $\mathbf{x}$  and is therefore not a free energy at all! It is instead a free-energy density and will be denoted by lower case  $f(m(\mathbf{x}))$ . To get the total free energy, which describes the whole system,  $f$  is integrated over space:

$$F = \int f(m(\mathbf{x})) d\mathbf{x}. \quad (154)$$

Note that  $F$  depends on the magnetisation  $m(\mathbf{x})$ , but not in a straight-forward way. Instead, the entire configuration (or function)  $m(\mathbf{x})$  gives a single number for  $F$ . The terminology is that  $F$  is a functional of  $m(\mathbf{x})$ , and this dependence is denoted by  $F[m(\mathbf{x})]$ , with square brackets.

The outcome of the Landau-Ginzburg theory is to construct the free energy  $F[m(\mathbf{x})]$  via the free-energy density  $f(m(\mathbf{x}))$ . This outcome, the Landau-Ginzburg free energy, behaves more like a microscopic configuration energy than a true free energy (and is sometimes called the Landau-Ginzburg Hamiltonian). What this means is that we can use  $f(m(\mathbf{x}))$  as a starting point in calculating physical observables for this model. Note how different this is from a standard microscopic approach. There is no need to write down the microscopic degrees of freedom, but instead a functional is constructed based on symmetry arguments. This approach reflects the more general concept of universality.

Putting all of this together, the partition function for this Landau-Ginzburg theory for the O(N) model has the form

$$Z = \int [Dm_i(\mathbf{x})] e^{-\beta F[m_i(\mathbf{x})]}, \quad (155)$$

where  $\int [Dm_i(\mathbf{x})]$  is the sum over microstates. Because the set of microstates is now the set of functions  $m_i(\mathbf{x})$ , this sum is denoted by a type of integral called a functional integral. The Landau-Ginzburg free-energy density is given by

$$f = rm^2(\mathbf{x}) + um^4(\mathbf{x}) + c \sum_{ij} \nabla_i m_j(\mathbf{x}) \nabla_i m_j(\mathbf{x}). \quad (156)$$

Similarly, for nematic liquid crystals, the partition function has the form

$$Z = \int [DQ_{ij}(\mathbf{x})] e^{-\beta F[Q_{ij}(\mathbf{x})]}, \quad (157)$$

with  $f$  given by

$$f = rS(\mathbf{x})^2 + wS(\mathbf{x})^3 + uS(\mathbf{x})^4 + c \sum_{ijk} \nabla_i Q_{jk}(\mathbf{x}) \nabla_i Q_{jk}(\mathbf{x}). \quad (158)$$

This is the starting point for statistical field theory, the language used to understand universality and the renormalisation group in a rigorous and general way. These functional integrals can be evaluated in some cases, either exactly or using approximations, series expansions, etc... However, we will avoid doing any functional integration and examine the outcomes of statistical field theory in a phenomenological way instead.

### 10.3 Goldstone's theorem

Goldstone's theorem states that for every broken continuous symmetry, the system will exhibit a low-energy mode. This does not apply to the Ising model: the symmetry broken is up-down or discrete. However, for O( $N$ ) models with  $N > 1$ , the symmetry broken is a continuous rotational symmetry. One heuristic argument for Goldstone's theorem is to consider long-wavelength fluctuations in the vector (or tensor) order parameter. For example, for  $N = 2$ , consider the angle of the magnetisation vector  $\mathbf{m} = m(\cos \theta, \sin \theta)$ . In the absence of an external field, changing the angle  $\theta$  does not cost any energy (because the energy depends only on  $m$ ). A low-energy mode can be constructed by varying  $\theta$  slowly in space. If the variations have lengthscale  $L$ , then the associated energy cost is  $O(\theta^2/L^2)$ , and goes to zero as  $L$  become larger. These can be represented as long-wavelength sinusoidal modes.

Physically, examples include the transverse sound modes in crystalline solids (whose presence is also the reason that solids are rigid). In magnets, such modes are called spin-waves.

The reason that the  $N = 2$  mode has exactly one such angle  $\theta$  is because only one continuous symmetry (two-dimensional rotation) is spontaneously broken. This argument applies for every continuous broken symmetry, except...

### 10.4 Anderson-Higgs mechanism

Goldstone's theorem excludes certain types of combinations of broken symmetries that are closely tied together. One example is again the case of crystalline solids: these solids break six symmetries total (three translational + three rotational), but exhibit only three Goldstone modes (three acoustic modes). For two-dimensional solids, there are two Goldstone modes. Why do the rotations not count for this argument?

The reason is that these broken symmetries are not independent. Instead, breaking the translation symmetries also affects the rotational modes, which are then gapped (i.e., cost a finite amount of energy to excite independently, even in the long-wavelength limit). The more general

argument has to do with what are called gauge symmetries (rather than global symmetries like rotation or translation). This argument also applies to particles in high-energy physics, where the analogous phenomena are massive particles (corresponding to gapped modes) that arise as a result of a broken gauge symmetry coupled to another broken-symmetry field. This led to the prediction of the Higgs boson (as an excitation of the broken symmetry field) by observations that some particles corresponding to the gauge symmetries (so-called W and Z bosons) have mass.